Clinical & Experimental Immunology
The Journal of Translational Immunology
immunology
Clinical and Experimental Immunology ORIGINAL ARTICLE doi:10.1111/j.1365-2249.2008.03816.x

B cells play a crucial role as antigen-presenting cells and collaborate with inflammatory cytokines in glucose-6-phosphate isomerase-induced arthritis

Y. Tanaka-Watanabe,* I. Matsumoto,*† K. Iwanami,* A. Inoue,* D. Goto,* S. Ito,* A. Tsutsumi* and T. Sumida*
*Division of Clinical Immunology, Major of Advanced Biomedical Applications, Graduate School of Comprehensive Human Sciences, University of Tsukuba, Tennodai, Tsukuba, and †PRESTO, Japan Science and Technology Agency, Honcho Kawaguchi, Saitama, Japan

Accepted for publication 8 October 2008
Correspondence: I. Matsumoto, Division of Clinical Immunology, Advanced Biomedical Applications, Graduate School of Comprehensive Human Sciences, University of Tsukuba, 1-1-1 Tennodai, Tsukuba 305-8575, Japan.
E-mail: ismatsu@md.tsukuba.ac.jp

Summary

Anti-glucose-6-phosphate isomerase (GPI) antibodies from K/BxN mice directly induce arthritis; however, the transfer of these antibodies from mice with GPI-induced arthritis does not induce arthritis. $CD4^+$ T cells play an important role in the induction and effector phase in this model; however, the roles of B cells and immunoglobulins (Igs) have not been elucidated. We investigated the roles of B cells and Igs in GPI-induced arthritis by using adoptive transfer system into SCID mice. Transfer of splenocytes of male DBA/1 mice immunized with GPI into SCID mice induced arthritis on day 6 in the latter, in association with the production of anti-GPI antibodies. Co-localization of C3 and IgG on the articular surface was identified in arthritic SCID mice. Inoculation of IgG (or anti-GPI antibodies) and $CD19^+$-depleted splenocytes from arthritic DBA/1 mice induced arthritis in SCID mice, but not $CD19^+$-depleted or $CD4^+$-depleted splenocytes from DBA/1 mice. *In vitro* analysis of cytokine production by splenocytes from DBA/1 arthritic mice demonstrated production of large amounts of tumour necrosis factor (TNF)-α and interleukin (IL)-6 in an antigen-specific manner ($P < 0.01$), and production was dominated by $CD19^+$-depleted than $CD4^+$-depleted splenocytes ($P < 0.05$). Addition of IgG from DBA/1 arthritic mice to the culture enhanced TNF-α but not IL-6 production, and this effect was blocked by anti-Fcγ receptor antibody. *In vivo* analysis of neutralization with TNF-α protected arthritis completely in SCID mice. Our results highlight the important role of B cells in GPI-induced arthritis as autoantibody producers, and these autoantibodies can trigger joint inflammation in orchestration with inflammatory cytokines, especially TNF-α.

Keywords: animal model, autoantibodies, B cell, glucose-6-phosphate isomerase, rheumatoid arthritis

Introduction

Rheumatoid arthritis (RA) is a common chronic autoimmune disease of unknown aetiology characterized by progressive inflammatory process and destruction of joints. Several autoantigens play a role in arthritis [1], and one of the candidate arthritogenic antigens, glucose-6-phosphate isomerase (GPI), was identified in the K/BxN model of arthritis [2]. GPI is a ubiquitous cytoplasmic enzyme, and anti-GPI antibodies in K/BxN mice induce arthritis directly. The effector mechanisms of anti-GPI antibodies have been confirmed by the requirement of innate immune system players, e.g. complement cascade, FcγR, especially FcγRIII, neutrophils and mast cells [3–6]. In addition, GPI accumulates on the synovium and joint articular surfaces, and the formation of a specific immunocomplex on the joint cavity leads ultimately to arthritis in the K/BxN serum transfer model [7]. These results indicate that ubiquitous antigens might be the targets of arthritogenic antibodies.

Recent studies have reported that immunization of DBA/1 mice with human GPI provoked arthritis, supporting the notion that autoimmunity to GPI plays a direct role in arthritis in genetically unaltered mice [8,9]. $CD4^+$ T cells were necessary for both the induction and the effector phase of the disease because arthritis was ameliorated by depletion of $CD4^+$ T cells with anti-CD4 monoclonal antibodies (mAbs). On the other hand, the role of B cells in this form of arthritis is still obscure. Immunoglobulin (Ig)G purified

from arthritic DBA/1 mice did not induce arthritis in naive DBA/1 mice; however, $Fc\gamma R^{-/-}$ mice developed mild arthritis following GPI immunization [8]. Moreover, both B cell-deficient C3H.Q and B10.Q mice are resistant to GPI-induced arthritis [9]. These results suggest that GPI-induced arthritis is B cell-dependent, although it is not clear that these cells are required as autoantibody-producing cells similar to antigen-presenting cells (APCs).

In the present study, we assessed the role of B cells and Igs in GPI-induced arthritis in DBA/1 mice using adoptive transfer into immunodeficient SCID mice. SCID mice were inoculated with splenocytes from GPI-immunized DBA/1 mice plus GPI. They developed arthritis with evident immune complex activation on the articular surface. Splenocytes lacking B and $CD4^+$ T cells from arthritic DBA/1 mice failed to induce arthritis in SCID mice. SCID mice recipients of both IgG (or purified anti-GPI antibodies) from GPI immunized DBA/1 mice and B cell-depleted splenocytes developed arthritis, whereas SCID mice recipients of IgG (or anti-GPI antibodies) only did not. Moreover, *in vitro* analysis of splenocytes of arthritic mice showed production of tumour necrosis factor (TNF)-α and interleukin (IL)-6 in an antigen-specific manner, driven mainly by B cell-depleted splenocytes. TNF-α, in particular, was produced mainly by $CD11b^+$ cells. *In vivo* neutralization of TNF-α protected arthritis development of SCID mice completely. These results suggest that B cells play a crucial role as antibody producers, and that antigen-induced cytokine production, especially TNF-α, seems to enhance the development of GPI-induced arthritis.

Materials and methods

Induction of GPI-induced arthritis in DBA/1 mice

Male DBA/1 mice (6–8 weeks old) were obtained from Charles River Laboratories (Yokohama, Japan). Recombinant human GPI was prepared as described previously [10]. Mice ($n = 10$) were immunized by intradermal injection of 300 μg of recombinant human GPI-gluthathione S-transfererase (GST) (hGPI) in emulsified Freund's complete adjuvant (CFA) (Difco, Detroit, MI, USA). As a control, we immunized another group of DBA/1 mice ($n = 10$) with 300 μg of GST in CFA. The experimental protocol was approved by the Ethics Review Committee for Animal Experimentation of Tsukuba University.

Arthritic animals were assessed clinically and ankle thickness was recorded. We used the following arthritis scoring system to evaluate the disease state (clinical score): 0 = no evidence of inflammation, 1 = subtle inflammation or localized oedema, 2 = easily identified swelling but localized to either dorsal or ventral surface of paws and score 3 = swelling on all aspects of paws. All four limbs were evaluated, yielding a maximum possible score of 12 per mouse.

Human recombinant GPI/GST fusion protein was produced by *Escherichia coli* with pGEX vector (GE Healthcare, Uppsala, Sweden), as described previously [2]. GPI/GST fusion protein was purified from lysate with gluthathione sepharose 4B (GE Healthcare). The volume of GPI/GST fusion proteins was determined at 280 nm and the purity of proteins checked using standard sodium dodecyl sulphate gels.

Induction of arthritis in SCID mice

CB17/ICR-*Prkdc*^{scid} (SCID) mice (8–10 weeks old) were purchased from Charles River Laboratories. The spleens were removed from arthritic DBA/1 mice on day 14 after immunization. The harvested splenocytes were suspended in phosphate-buffered saline (PBS) and erythrocytes were lysed. The remaining cells were washed in PBS, then separated by magnetic affinity cell sorting (MACS; Militenyi Biotech, Bergisch Gladbach, Germany) using anti-$CD4^+$ (T cells) or anti-$CD19^+$ (B cells)-depleted splenocytes, estimated by fluorescence activated cell sorter (FACS) (> 99% cells were depleted). These cells were inoculated intraperitoneally with 100 μg GPI into SCID mice.

Enzyme-linked immunosorbent assay

The enzyme-linked immunosorbent assay (ELISA) microtitre plates were coated with 5 μg/ml rh-GPI in PBS (Sumitomo Bakelite, Tokyo, Japan) overnight at 4°C. The plates were then washed and saturated with 300 μl blocking solution (Dainippon Sumitomo Pharma, Tokyo, Japan) at room temperature. After 2 h, they were washed and 1/500 diluted serum with blocking solution was added. Incubation was carried out for 2 h at room temperature. The plates were washed and 150 μl alkaline phosphatase-conjugated Fc-specific anti-mouse IgG antibody (American Qualex, San Clemente, CA, USA) diluted at 1:5000 with blocking solution was added. After incubation at room temperature for 1 h, the plates were detected with 150 μl of substrate solution (9·6% 2-aminoethanol, 2·4 mM $MgCl_2$ in distilled and deionized water, pH 9·8). Colour development was read by a microplate reader at 405 nm.

Antibody purification

Antibodies were purified from sera of DBA/1 mice immunized with 300 μg rh-GPI or GST. Serum samples were diluted 10-fold with binding buffer and then poured over a protein G column (GE Healthcare, Uppsala, Sweden) to purify IgG. Anti-GPI antibodies were also purified by affinity column (GE Healthcare), following the method described [2]. Purified antibodies were changed buffer to PBS by centricon YM-50 (Millipore, Billerica, MA, USA).

Histological examination

Mice were killed and hind-paw joints were fixed with 4% paraformaldehyde at 4°C for 6 h. The method used for

decalcification was described previously [11]. The tissues were then embedded in optimal cutting temperature compound (Miles Scientific, Naperville, IL, USA) and frozen rapidly at −80°C. Frozen sections (5-μm thick) were cut on a cryostat and placed on magnesium aluminum silicate-coated glass microscope slides and allowed to air-dry. Joints were stained with haematoxylin and eosin (H&E) or fluorescent staining. Fluorescent antibodies were anti-C3 fluorescein isothiocyanate (FITC) (ICN Biomedicals, Solon, OH, USA) and anti-IgG Texas Red (EY Laboratories, San Meteo, CA, USA).

In vitro analysis of cytokine production by splenocytes from DBA/1 arthritic mice

Spleens were removed from arthritic GPI-induced mice on day 14. The spleens were harvested and haemolyzed with 0·83% NH_4Cl, 0·12% $NaHCO_3$ and 0·004% ethylenediamine tetraacetic acid 2Na in PBS. Single-cell suspensions were prepared in RPMI-1640 medium (Sigma-Aldrich, St Louis, MO, USA) supplemented with 10% FBS, 100 U/ml of penicillin, 100 μg/ml of streptomycin and 50 μM of 2-mercaptoethanol. $CD4^+$ T cells, CD11b cells, CD11c cells or $CD19^+$ cells were isolated and enriched by MACS (Miltenyi Biotech). The cell purity was confirmed by flow cytometry (> 90%). Whole splenocytes or MACS-separated cells (1×10^6 cells/ml) were cultured with 5 μg/ml of GPI (or GST) at 37°C in 5% CO_2 for 12 h. Anti-FcγR II/III receptor antibody (BD Bioscience, San Jose, CA, USA) was used at 1 μg/ml as an Fc blocker. Supernatants were assayed for TNF-α, interferon (IFN)-γ, IL-17 and IL-6 by Quantikine ELISA kit (R&D Systems, Minneapolis, MN, USA) or ELISA Ready-SET-Go! (eBioscience, San Diego, CA, USA).

In vivo analysis using mAb for neutralizing cytokines

We used commercially available anti-TNF-α mAbs (eBioscience) and anti-IL-6 mAbs (R&D Systems) to neutralize the respective cytokines. As a control antibody, we used the same amount of Rat IgG1 isotype control (R&D Systems). In SCID-transferred arthritis, each mouse received a single injection of 100 μg of anti-TNF-α mAb, anti-IL-6 mAb or control Ig was injected on the day of splenocytes transferred (day 0).

Statistical analysis

All data were expressed as mean ± standard error of the mean. Differences between groups were examined for statistical significance using the Mann–Whitney *U*-test. A *P*-value less than 0·05 denoted a statistically significant difference.

Results

The GPI-induced arthritis in DBA/1 mice

Arthritis was induced in DBA/1 mice with 300 μg rh-GPI emulsified in CFA. Beginning on day 8 after immunization, the paws and ankles of mice were examined daily for clinical signs of arthritis. Joint swelling reached maximum around day 14, then resolved gradually (Fig. 1a). Arthritic changes were observed mainly in the paws (Fig. 1b, right) and ankles of immunized DBA/1 mice, but not in digits. Control (GST) immunization did not lead to apparent arthritis (Fig. 1b,c, left). Histopathological examination showed synovium proliferation (Fig. 1c, right), resulting in bone destruction (data not shown). Immunohistochemical analysis confirmed co-localization of IgG and C3 on the surface of cartilage on day 14 in arthritic DBA/1 mice (Fig. 1d right; control immunization on left). These findings suggest that immune complex activation in local joints is involved in the development of GPI-induced arthritis.

Successful transfer of GPI-induced arthritis into immunodeficient mice

Splenocytes (1×10^7 cells) from arthritic DBA/1 mice were inoculated into SCID mice on day 14 post-immunization with 100 μg of GPI. Spleens from control SCID mice (Fig. 2a left) or SCID mice inoculated with splenocytes (1×10^7 cells) from arthritic DBA/1 mice (Fig. 2a right, on day 14) was shown. Arthritis developed in splenocyte-inoculated SCID mice (Fig. 2b right, c). However, arthritis was not observed in both SCID mice inoculated with the same number of splenocytes from arthritic DBA/1 mice without GPI, and SCID mice inoculated with splenocytes from naive DBA/1 mice with GPI (Fig. 2b left, c) These results indicate that splenocytes from arthritic mice plus GPI contain important factor(s) in the induction of arthritis.

Histological analysis of arthritic SCID mice

Histopathological examination of the arthritic joints of SCID mice showed synovial hyperplasia in arthritic SCID mice inoculated with splenocytes from arthritic DBA/1 mice (H&E staining, Fig. 3b,c), but not in SCID mice inoculated with splenocytes from naive DBA/1 mice (Fig. 3a). Immunohistochemical study showed co-localization of IgG and C3 on the cartilage surface of arthritic SCID mice (Fig. 3d), but not in joints of SCID mice inoculated with splenocytes from naive DBA/1 mice. These findings suggest that Igs produced by inoculated splenocytes from DBA/1 mice attach to the articular surface of SCID mice and result in arthritis by complement activation.

Importance of T and B cells in arthritis of SCID mice

To evaluate the role of $CD19^+$ or $CD4^+$ cells in arthritis of SCID mice, we inoculated 1×10^7 $CD19^+$- or $CD4^+$-depleted splenocytes of arthritic DBA/1 mice plus 100 μg of GPI into SCID mice. In these inoculi, the percentage of $CD19^+$ and $CD4^+$ cells in depleted splenocytes was less than 1%. Neither

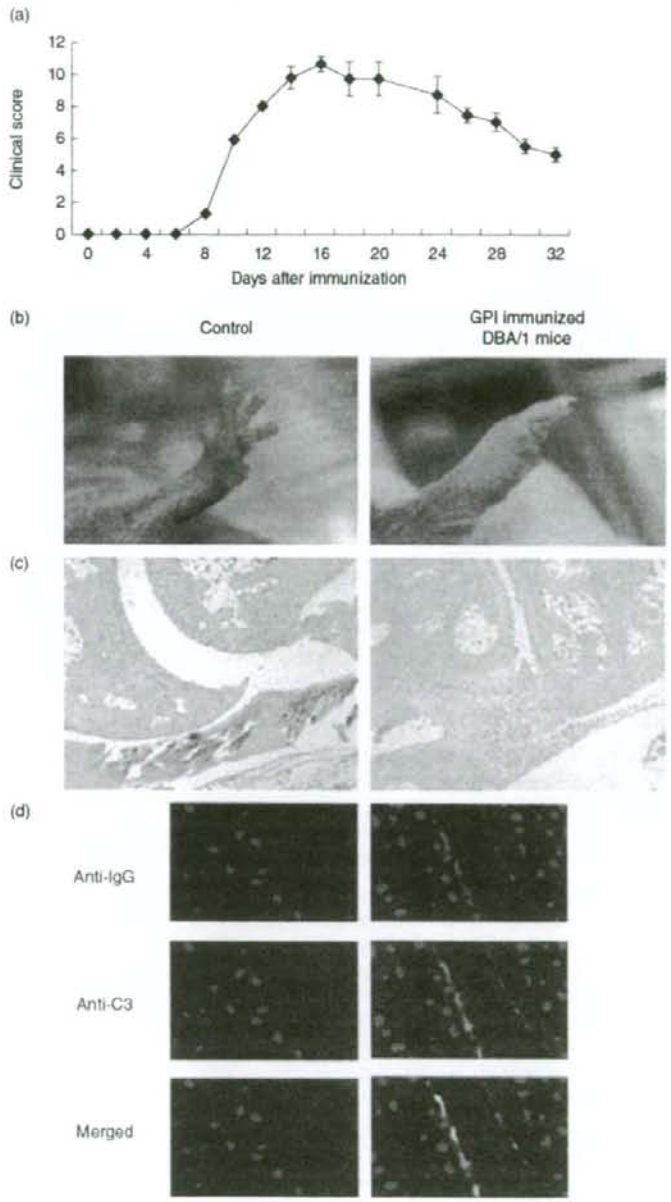

Fig. 1. Clinical and histological evaluation of glucose-6-phosphate isomerase (GPI)-induced arthritis in DBA/1 mice. Mean of clinical score (a) (±standard error of the mean, 10 mice) followed days after immunization. (b) Paw of control DBA/1 mouse treated with control antigens [gluthathione S-transfererase (GST)] 300 μg (left). DBA/1 mice were immunized with rh-GPI 300 μg in Freund's complete adjuvant (CFA) (right). (c) Histological examination of ankle joints of the control (left) and GPI-induced arthritis on day 14 showing severe synovium proliferation (haematoxylin and eosin staining, right). (d) Anti-C3 (green) and anti-immunoglobulin (Ig)G (red) staining in joints of control (left) and arthritic DBA/1 mice (right). Nuclei were counterstained with 4,6-diamino-2-phenylindole (blue). C3 and IgG were co-localized on the surface of cartilage of ankle joints (right). Magnification of original photographs: ×40 (c) or ×600 (d); spl: splenocytes.

$CD19^+$ nor $CD4^+$ cell-depleted splenocytes induced arthritis in SCID mice (Fig. 4a), or produced anti-GPI antibodies (Fig. 4b), suggesting that both $CD19^+$ and $CD4^+$ cells play important roles in the induction of arthritis in SCID, and that production of anti-GPI antibodies may be indispensable for such induction.

Importance of B cells as producers of antibodies in arthritis of SCID mice

It has been reported previously that B cell-deficient mice are resistant to GPI-induced arthritis [9]. However, whether these cells act as autoantibody-producing cells as well as APCs

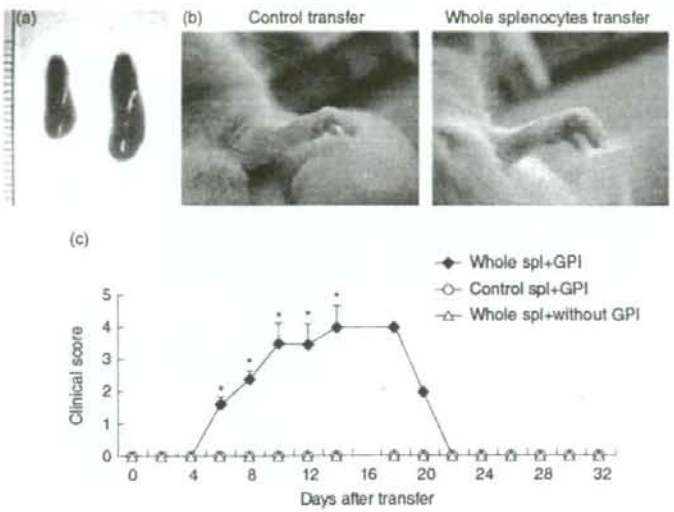

Fig. 2. Transfer of arthritis in SCID mice. Glucose-6-phosphate isomerase (GPI)-immunized DBA/1 mice were killed on day 14, and 1×10^7 splenocytes (spl) were isolated and transferred into SCID mice with 100 μg of GPI. (a) Spleen of control SCID mice (left) and SCID mice inoculated with splenocytes of arthritic DBA/1 mice 1×10^7 cells (right on day 14). (b) Feet of SCID mice inoculated with splenocytes from naive DBA/1 mice (left) and SCID mice inoculated with splenocytes from GPI-induced arthritic DBA/1 mice (right). (c) Clinical score and development of arthritis in SCID mice. Swelling of paws was observed on day 6 in SCID mice inoculated with whole splenocytes plus 100 μg of GPI (◆). Control mice were inoculated with 1×10^7 splenocytes only from immunized DBA/1 mice (△) or 1×10^7 splenocytes from control immunized DBA/1 mice plus 100 μg of GPI (○). Control mice did not develop arthritis. Data are mean ± standard error of the mean of five mice in each group. $^*P < 0.05$ by Mann–Whitney *U*-test.

is unknown at present. To investigate the role of autoantibodies, we inoculated SCID mice with IgGs from arthritic DBA/1 mice. IgGs were purified from the sera of DBA/1 mice on day 14 after immunization. Injection of 3 mg IgG alone from arthriticDBA/1 mice did not result in overt arthritis in SCID mice, even if we added 100 μg of GPI (Fig. 5a). However, injection of IgG with $CD19^+$-depleted splenocytes and GPI resulted in the development of arthritis in SCID mice (Fig. 5a). To investigate further the arthritogenicity of anti-GPI antibodies, we used affinity purified anti-GPI antibodies from arthritic DBA/1 mice. Injection of 3 mg anti-GPI antibodies alone did not result in arthritis in SCID mice, even if we added 100 μg of GPI (Fig. 5b). However, with $CD19^+$-depleted splenocytes, even if we used 1mg of affinity purified anti-GPI antibodies from GPI-induced mice instead of IgG, clear arthritis was developed in SCID mice (Fig. 5b). These findings suggest that $CD19^+$ cells play an important role as producers of antibody (especially anti-GPI antibodies) in arthritis of SCID mice; however, anti-GPI antibodies alone from GPI-induced arthritis do not have arthritogenecity.

Importance of TNF-α in the development of arthritis in SCID mice

To determine the humoral factors that were mediated by arthritis with splenocytes from GPI-induced arthritis plus GPI in SCID mice, we screened *in vitro* cytokine production from splenocytes plus GPI. We selected two proinflammatory cytokines in these experiments based on the preliminary results of cytometric beads array analysis, which revealed antigen-specific expression of TNF-α and IL-6 (data not shown); they have recently proved to be important in the induction of GPI-induced arthritis [12]. Indeed, the addition of GPI to the culture medium induced the production of large amounts of TNF-α and IL-6, while control antigen did not induce these cytokines (Fig. 6a). We also examined the production of these cytokines by $CD19^+$- and $CD4^+$-depleted cells. TNF-α and IL-6 levels were enhanced in the presence of $CD19^+$-depleted cells compared with $CD4^+$-depleted cells (Fig. 6a), and enriched slightly in $CD19^+$-depleted cells compared with whole splenocytes. To examine the role of IgG from DBA/1 arthritic mice, $CD19^+$-depleted splenocytes were stimulated with GPI and/or IgG *in vitro*. IgG triggered weak production of TNF-α and Fcγ blockade suppressed TNF-α production (Fig. 6b, $P < 0.05$). On the other hand, IL-6 production was regulated by neither IgG nor Fcγ blockade (Fig. 6b). To confirm the dependency of these inflammatory cytokines of arthritis in SCID mice, neutralizing mAbs were injected *in vivo* on the day of inoculation of splenocytes. Surprisingly, anti-TNF-α mAb protected arthritis completely in SCID mice, whereas anti-IL-6 mAb blocked arthritis partially (Fig. 6c). These findings suggest

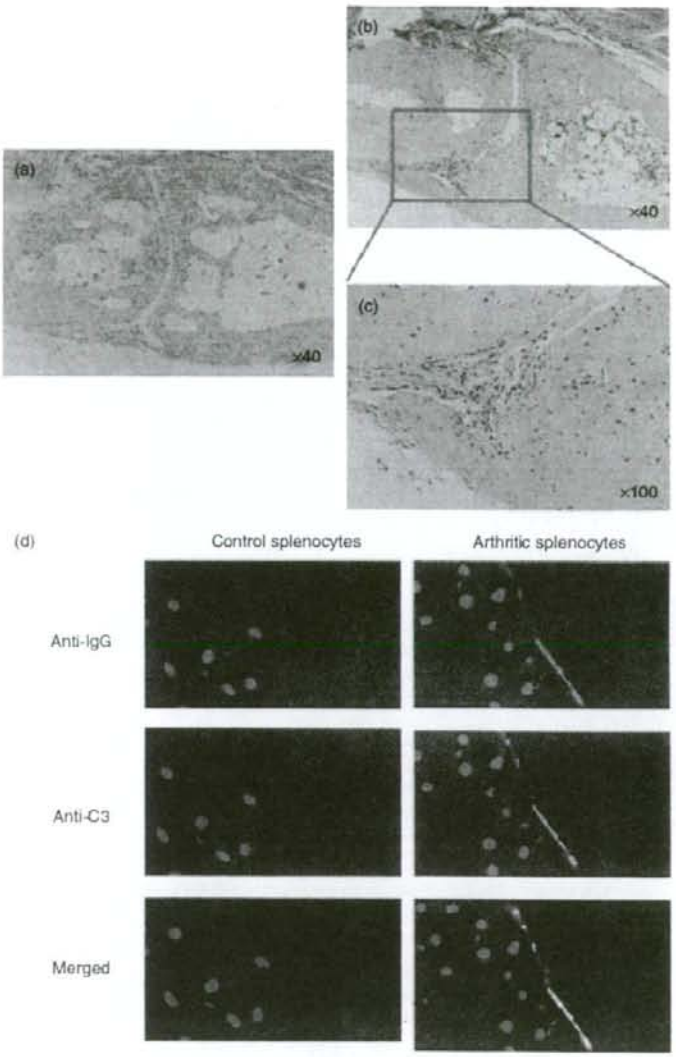

Fig. 3. Histological evaluation of joints of SCID mice. Joints of control mice inoculated splenocyte (spl) from naive DBA/1 mice with 100 μg of glucose-6-phosphate isomerase (GPI). (b,c) Synovial hyperplasia in a representative SCID mouse inoculated with splenocytes from arthritic DBA/1 mice. (d, right) Co-localization of immunoglobulin (Ig)G (red) and C3 (green) on the articular surface of SCID mice on day 14 after transfer by fluorescent staining. Nuclei were counterstained with 4,6-diamino-2-phenylindole (blue). Magnification of original photographs: ×40 (a), ×100 (b, c) or ×600 (d).

that TNF-α in particular (partially IL-6) induced by GPI may contribute to the development of arthritis, although IgG from arthritic mice contributed weakly to the production of TNF-α via Fcγ receptors.

CD11b$^+$ cells collaborating with CD4$^+$ T cells produce predominantly TNF-α

To analyse further the dominant cell populations that can produce TNF-α and IL-6, MACS-separated cells were co-cultured with GPI or GST (Fig. 7a,b). TNF-α was produced by several cell populations, driven mainly by CD11b$^+$ cells (Fig. 7a). It is possible that TNF-α production from CD11b cells was induced by the collaboration of activated T cells containing CD11b when cultured with GPI. On the other hand, IL-6 was produced predominantly by CD11c$^+$ cells (Fig. 7b). This cytokine production was enhanced by adding CD4$^+$ cells ($P < 0{\cdot}05$), thus CD4$^+$ T cells might also contribute for producing inflammatory cytokines.

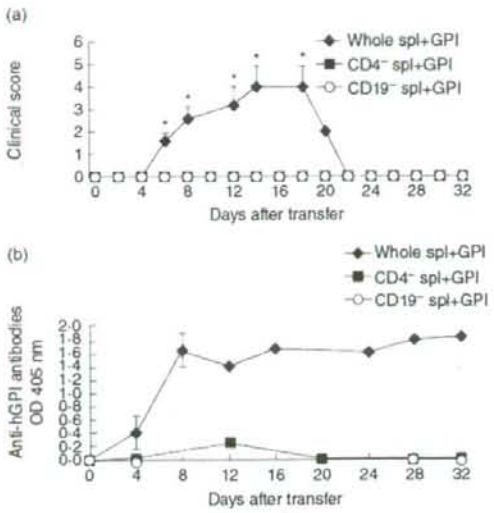

Fig. 4. Importance of anti-GPI antibodies in transfer of arthritis. CD19-depleted or CD4⁺-depleted splenocytes (spl) from arthritic DBA/1 mice obtained on day 14 after immunization were inoculated with glucose-6-phosphate isomerase (GPI) into SCID mice. (a) Mean clinical score. (b) Anti-GPI antibodies detected by enzyme-linked immunosorbent assay (ELISA) at 405 nm (b). (◆) SCID mice that received 1×10^7 of splenocytes from arthritic DBA/1 mice plus 100 μg GPI; (■) SCID mice recipients of 1×10^7 CD4⁺-depleted cells plus 100 μg GPI; (○) SCID mice recipients of 10^7 CD19-depleted cells plus 100 μg GPI. Data are mean ± standard error of the mean of five mice in each group. *$P < 0.05$ by Mann–Whitney U-test.

Exploring antigen-presenting function of B cells

Finally, to evaluate B cell function as APCs, MACS-separated CD4⁺ T cell and CD19⁺ cells were co-cultured with GPI. IFN-γ and IL-17 production were used to indicate the barometer of the antigen presentation function of B cells. Both IFN-γ and IL-17 were up-regulated clearly by adding CD19⁺ splenocytes ($P < 0.05$), indicating that CD19⁺ cell may function as APCs (Fig. 7c,d).

Discussion

Anti-GPI antibodies from K/BxN mice are well known as arthritogenic autoantibodies, and their effector mechanisms have been identified in several elegant studies [2–7]. Briefly, the key players involved in the development of arthritis after the transfer of anti-GPI antibodies included Fcγ receptor (particularly FcγRIII), alternative complement pathways such as factors B, C3, C5 and C5aR [3], subsets of Fcγ receptor or C5a receptor-bearing cells [4–6] and some inflammatory cytokines such as IL-1 and TNF-α [3]. In particular, a dominant pathological action driven by anti-GPI antibodies is a local association between GPI and anti-GPI on the articular surface, which leads to complement activation in the joints [7,13].

However, anti-GPI antibodies from GPI-induced arthritis did not induce overt arthritis in naive mice [8]. A previous report showed that B cell-deficient C3H.Q and B 10.Q mice were resistant to GPI-induced arthritis [9]. Moreover, FcγR-deficient mice were protected from GPI-induced arthritis, whereas mice deficient in inhibitory FcγRIIB developed severe arthritis [8]. These results show that B cells play an essential role in arthritis by producing autoantibodies that

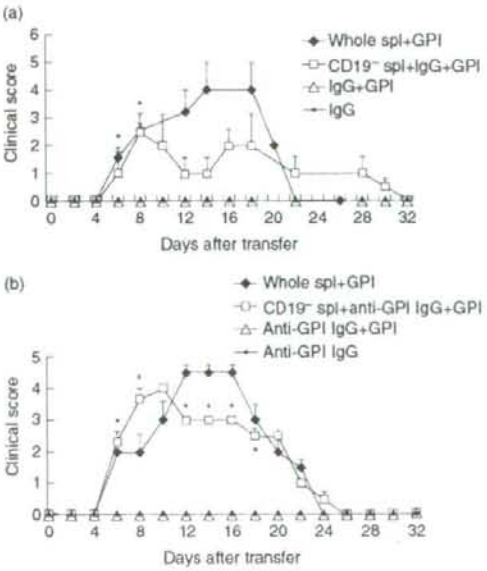

Fig. 5. Role of B cells in induction of arthritis in SCID mice. IgG from arthritic DBA/1 mice (alone or with glucose-6-phosphate isomerase (GPI)) or immunoglobulin (Ig)G plus CD19⁺-depleted cells were inoculated into SCID mice. Development of arthritis in SCID mice was monitored. (a) Mean clinical score is depicted. (◆) SCID mice that received 1×10^7 splenocytes (spl) plus 100 μg GPI; (□) SCID mice recipients of 1×10^7 CD19-depleted cells from arthritic DBA/1 mice with 3 mg of IgG plus 100 μg of GPI; (△) SCID mice recipients of 3 mg of IgG from arthritic DBA/1 mice plus 100 μg GPI; (•) SCID mice recipients of 3 mg of IgG from arthritic DBA/1 mice alone. (b) Affinity purified anti-GPI antibodies from arthritic DBA/1 mice (alone or with GPI), or anti-GPI antibodies plus CD19⁺-depleted cells were inoculated into SCID mice and monitored. (◆) SCID mice that received 1×10^7 spenocytes plus 100 μg GPI; (□) SCID mice recipients of 1×10^7 CD19-depleted cells from arthritic DBA/1 mice with 1 mg of anti-GPI antibodies plus 100 μg of GPI; (△) SCID mice recipients of 3 mg of anti-GPI antibodies from arthritic DBA/1 mice plus 100 μg GPI; (•) SCID mice recipients of 3 mg of anti-GPI antibodies from arthritic DBA/1 mice alone. Data are mean ± standard error of the mean of five mice in each group. *$P < 0.05$ by Mann–Whitney U-test.

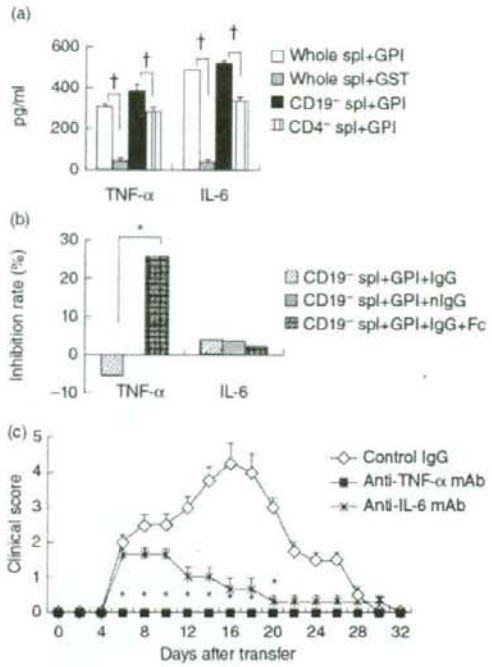

Fig. 6. *In vitro* cytokine production by splenocytes from arthritic DBA/1 mice and *in vivo* neutralization of inflammatory cytokines in SCID mice. Cytokine concentrations in supernatant of cultured splenocytes (spl) from arthritic DBA/1 mice were assessed by enzyme-linked immunosorbent assay. (a) Whole splenocytes or separated splenocytes (10^6 cell/ml) were cultured with 5 μg/ml of glucose-6-phosphate isomerase (GPI) or gluthathione S-transfererase (GST). (b) $CD19^+$-depleted splenocytes were cultured with GPI and immunoglobulin (Ig)G with/without FcγR blocker. IgG was purified from arthritic DBA/1 mice on day 14 after GPI immunization. Naive IgG (nIgG) was purified from naive DBA/1 mice. Inhibition rate was calculated to be divided by amount of productions from $CD19^+$-depleted splenocytes stimulated with GPI. Representative data of three independent experiments with three individual mice per experiment. (c) Neutralization of inflammatory cytokines was performed *in vivo* by monoclonal antibody (mAb), five mice in each group. SCID mice recipients of 1×10^7 splenocytes from arthritic DBA/1 mice plus 100 μg GPI and 100 μg of control IgG (◇), anti-tumour necrosis factor (TNF)-α mAb (■) or anti-interleukin (IL)-6 mAb (*). Data are mean ± standard error of the mean of five mice in each group. $^*P < 0{\cdot}05$, $^\dagger P < 0{\cdot}01$, by Mann–Whitney *U*-test.

result in FcγR activation in this model. In our immunohistological study, a clear complement activation by immune complex was observed in joints of mice with GPI-induced arthritis. This finding suggests that local immune complex (probably GPI–anti-GPI antibodies) activation in the joints also plays an important role in GPI-induced arthritis.

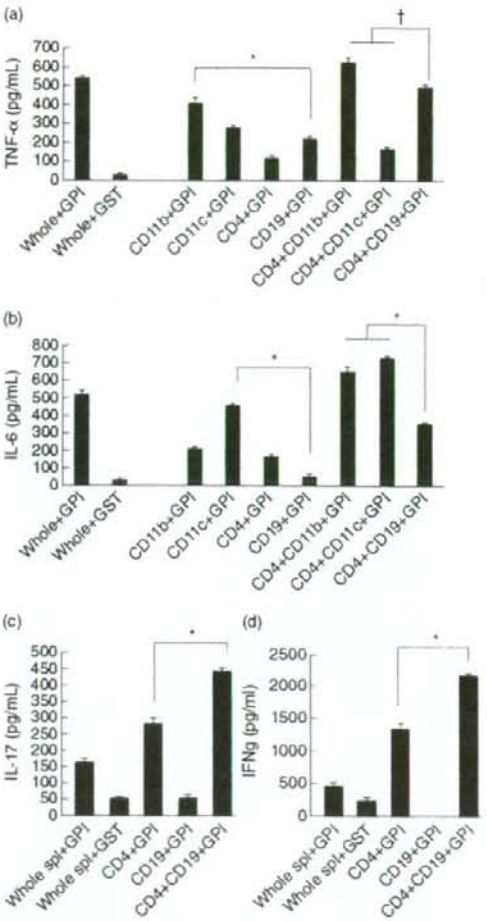

Fig. 7. Exploration of dominant cell population of inflammatory cytokines, and B cell functions as an antigen-presenting cells (APCs) *in vitro*. Whole splenocytes (spl) or independent magnetic affinity cell sorting (MACS) separated ($CD4^+$, $CD19^+$, $CD11b^+$ and $CD11c^+$ cells) splenocytes (total 1×10^6 cells/ml) were cultured with 5 μg/ml of glucose-6-phosphate isomerase (GPI) or gluthathione S-transfererase (GST). Inflammatory cytokines [tumour necrosis factor (TNF)-α (a) and interleukin (IL)-6 (b)] and T cell-secreted cytokines [IL-17 (c) and interferon (IFN)-γ (d)] were compared between $CD19^+$ cells and other APCs ($CD11b^+$ $CD11c^+$ cells). Cytokine concentrations in supernatant of cultured splenocytes from arthritic DBA/1 mice were assessed by enzyme-linked immunosorbent assay. The purity of cells was estimated by fluorescence activated cell sorter flow cytometry (> 90%). Data are mean ± standard error of the mean of three mice in each group. $^*P < 0{\cdot}05$, $^\dagger P < 0{\cdot}001$, by Mann–Whitney *U*-test.

To determine the role of B cells more precisely, we set up a transfer system using SCID mice. SCID mice inoculated with splenocytes from GPI-immunized DBA/1 mice together with GPI developed arthritis, and the immune complex activation was also noted on the articular surface of SCID mice. In GPI-induced arthritis, the expression of TNF-α mRNA in inflammatory joints and serum was increased on day 7 when detectable amounts of anti-GPI antibodies were produced (reference [12] and our unpublished data). B cell-depleted splenocytes from arthritic DBA/1 mice could not induce arthritis in SCID mice. On the other hand, SCID mice that received IgG (or anti-GPI antibodies) with B cell-depleted splenocytes from GPI-immunized DBA/1 mice developed arthritis, whereas SCID mice that received only IgG did not. These results suggest that B cells play a crucial role as antibody producers, followed by immune complex deposition on the articular surfaces in arthritis.

Our scenario is similar to adoptive transfer of collagen-induced arthritis (CIA) to SCID mice [14–16]. However, the GPI-induced arthritis in SCID mice occurred earlier (5–6 days) than CIA (14–16 days). The other difference between these two types of arthritis is that IgG from GPI-induced arthritis did not have arthritogenic capacity, whereas CIA IgG alone exhibit such capacity. Thus, anti-GPI antibodies produced by inoculated splenocytes play an important role in the induction of arthritis. However, these antibodies could not induce arthritis when injected alone, and thus we need to know about other humoral factors that trigger arthritis.

Our *in vitro* assay with splenocytes from GPI-induced arthritis plus GPI indicated that TNF-α and IL-6 may be crucial for the induction of arthritis. An earlier study from our laboratories identified the therapeutic efficacy of both anti-TNF-α mAb and anti-IL-6 mAb in GPI-induced arthritis [12]. Moreover, we clearly confirmed a protective effect of anti-TNF-α mAb in SCID-transferred arthritis. These results indicate that arthritis in SCID recipients may be enhanced mainly not only by anti-GPI antibodies, but also humoral factors such as TNF-α and IL-6. In particular, the development of arthritis was associated with the production of anti-GPI antibodies in SCID mice, thus autoantibodies might play a crucial role especially in the local joints, collaborating with inflammatory cytokines.

Concerning the other role of B cells, our *in vitro* assay suggests that B cells had a weak capacity of producing TNF-α, as well as antigen-presenting function with GPI culture. A recent paper reported that subsets of dendritic cells (DC) could express CD19 [17], thus it is possible that these cells comprise such functions of B cells. However, we tested *in vivo* experimentally with $CD19^+$-depleted cells, suggesting that the antoantibody produced indeed contributed to the development of arthritis.

What is the role of T cells in GPI-induced arthritis? Based on our experiments, splenocytes lacking $CD4^+$ cells failed to induce arthritis in SCID mice. The lack of anti-GPI antibodies in the serum of SCID recipients of the $CD4^+$ T cell-depleted cell population suggests that production of autoantibodies is $CD4^+$ T cell-dependent. Moreover, our *in vitro* assay identified $CD19^+$-depleted cells (probably comprising APCs plus T cells) as the main source of inflammatory cytokines that can trigger arthritis. TNF-α and IL-6 production was enhanced by adding $CD4^+$ cells, as confirmed by *in vitro* assay. In this regard, in GPI-induced arthritis, administration of anti-CD4 mAb on days 11 and 14 after immunization induced rapid remission of the arthritis [8]. We have reported previously that GPI-specific $CD4^+$ T cells were differentiated to T helper type 1 (Th1) and Th17 [18]. The administration of anti-IL-17 mAb on day 7 ameliorated arthritis significantly, whereas that administered on day 14 did not affect the disease. Moreover, *our vitro* assay using splenocytes on day 14 could detect tiny amounts of IL-17 with GPI ([17], and our unpublished data). These findings show that $CD4^+$ T cells (particularly Th17 cells) are necessary in the induction phase, and they function as supporters of production with autoantibodies and inflammatory cytokines in the effector phase of GPI-induced arthritis.

Are these scenarios relevant to human RA? High titres of anti-GPI antibodies are found in patients with severe forms of RA, but in only a few control individuals [10,19,20]. We reported recently that a *FCGR3A*-158V/F functional polymorphism was associated with RA in anti-GPI antibody-positive individuals, because 89% of healthy subjects positive for anti-GPI antibodies possessed homozygous low-affinity genotype *FCGR3A*-158F [21]. Moreover, among anti-GPI antibody-positive individuals, GPI-reactive $CD4^+$ T cells, especially Th1 cells, are detected specifically in peripheral blood mononucleocytes of patients with RA who share either human leucocyte antigen (HLA)-DRB1 *0405 or *0901 haplotypes [22]. These findings suggest that arthritis in anti-GPI antibody-positive individuals depends on several important factors, such as GPI-reactive T cells, HLA-DR*0405/*0901 and FcγRIII.

What of the role of anti-GPI antibodies in GPI-induced arthritis? The $H2^q$ haplotype confers severe form of arthritis [9]. High titres of anti-GPI antibodies were also found in arthritis-resistant C57BL/6($H2^b$) mice, although their T cells had weak GPI responses ([8], and our observations) compared with arthritis-susceptible DBA/1 mice. In addition, $Fc\gamma R^{-/-}$ mice are protected from GPI-induced arthritis, whereas $Fc\gamma RIIB^{-/-}$ mice developed pronounced arthritis [8]. These findings indicate that anti-GPI antibodies do not induce arthritis *per se*; it is probable that unique activation of major histocompatibility complex class II and antigen-specific T cells might be indispensable. In this regard, GPI-induced arthritis appears to be akin to human RA.

In conclusion, we identified that B cells play a crucial role in GPI-induced arthritis as autoantibody producers. This finding might explain how autoantibodies orchestrate the induction of arthritis with inflammatory cytokines such as TNF-α in patients with RA.

Acknowledgements

We thank Miss Yuri Ogamino for excellent technical assistance. This work was supported in part by a grant from the Japanese Ministry of Science and Culture (I. M., T. S.).

References

1 Kannann KR, Ortmann A, Kimpel D. Animal models of rheumatoid arthritis and their relevance to human disease. Pathophysiology 2005; **12**:167–81.

2 Matsumoto I, Staub A, Benoist C, Mathis D. Arthritis provoked by linked T and B cell recognition of glycolytic enzyme. Science 1999; **286**:1732–5.

3 Ji H, Ohmura K, Mahmood U *et al.* Arthritis critically dependent on innate immune system players. Immunity 2001; **16**:157–68.

4 Binstadt BA, Patel PR, Alencar H *et al.* Particularities of the vasculature can promote the organ specificity of autoimmune attack. Nat Immunol 2006; **7**:284–92.

5 Wipke BT, Allen PM. Essential role of neutrophils in the initiation and progression of a murine model of rheumatoid arthritis. J Immunol 2001; **167**:1601–8.

6 Lee DM, Friend DS, Gurish MF *et al.* Mast cells: a cellular link between autoantibodies and inflammatory arthritis. Science 2002; **297**:1689–92.

7 Matsumoto I, Maccioni M, Lee DM *et al.* How antibodies to ubiquitous cytoplasmic enzyme may provoke joint-specific autoimmune disease. Nat Immunol 2002; **3**:360–5.

8 Schubert D, Maier B, Moraweitz L *et al.* Immunization with glucose-6-phosphate isomerase induced T cell-dependent peripheral polyarthritis in genetically unaltered mice. J Immunol 2004; **172**:4503–9.

9 Bockermann R, Schubert D, Kamradt T *et al.* Induction of a B-cell-dependent chronic arthritis with glucose-6-phosphate isomerase. Arthritis Res Ther 2005; **7**:1316–24.

10 Matsumoto I, Lee DM, Goldbach-Mansky R *et al.* Low prevalence of antibodies to glucose-6-phosphate isomerase in patients with rheumatoid arthritis and a spectrum of other chronic autoimmune disorders. Arthritis Rheum 2003; **48**:944–54.

11 Mori S, Sawai T, Teshima T, Kyogoku M. A new decalcifying technique for immunohistochemical studies of calcified tissue, especially applicable to cell surface marker demonstration. J Histochem Cytochem 1988; **36**:111–4.

12 Matsumoto I, Zhang H, Yasukochi T *et al.* Therapeutic effects of antibodies to TNFalpha and IL-6 and CTLA-4 Ig in mice with glucose-6-phosphate isomerase-induced arthritis. Arthritis Res Ther 2008; **10**:R66.

13 Wipke BT, Wang Z, Nagengast W *et al.* Staging the initiation of autoantibody-induced arthritis: a critical role for immune complex. J Immunol 2004; **172**:7694–702.

14 Williams RO, Plater-Zyberk C, Williams DG, Maini RN. Successful transfer of collagen-induced arthritis to severe combined immunodeficient (SCID) mice. Clin Exp Immunol 1992; **88**:455–60.

15 Kadowaki KM, Matsuno H, Tsuji H, Tunru I. CD4$^+$ T cells from collagen-induced arthritic mice are essential to transfer arthritis into severe combined immunodeficient mice. Clin Exp Immunol 1994; **97**:212–8.

16 Taylor PC, Pleter-Zyverk C, Maini RN. The role of the B cells in the adoptive transfer of collagen-induced arthritis form DBA/1 (H-2^q) to SCID (H-2d) mice. Eur J Immunol 1995; **25**:763–9.

17 Baban B, Hansen AM, Chandler PR *et al.* A minor population of splenic dendritic cells expressing CD19 mediates IDO-dependent T cell suppression via type I IFN signaling following B7 ligation. Int Immunol 2005; **17**:909–19.

18 Iwanami K, Matsumoto I, Tanaka-Watanabe Y *et al.* Crucial role of IL-6/IL-17 cytokine axis in the induction of arthritis by glucose-6-phosphate isomerase. Arthritis Rheum 2008; **58**:754–63.

19 van Gaalen FA, Toes RE, Ditzel HJ *et al.* Association of autoantibodies to glucose-6-phosphate isomerase with extraarticular complications in rheumatoid arthritis. Arthritis Rheum 2004; **50**:395–9.

20 Kassahn D, Kolb C, Solomon S *et al.* Few human autoimmune sera detect GPI. Nat Immunol 2002; **3**:411–2.

21 Matsumoto I, Zhang H, Muraki Y *et al.* A functional variant of Fcg receptor IIIA is associated with rheumatoid arthritis in anti-glucose-6-phosphate isomerase antibodies-positive individuals. Arthritis Res Ther 2005; **7**:1183–8.

22 Kori Y, Matsumoto I, Zhang H *et al.* Characterization of Th1/Th2 type, glucose-6-phosphate isomerase reactive T cells in the generation of rheumatoid arthritis. Ann Rheum Dis 2006; **65**:968–9.

Visfatin (pre-B cell colony-enhancing factor) gene expression in patients with rheumatoid arthritis

Visfatin, also known as pre-B cell colony enhancing factor, is a cytokine-like protein originally cloned from peripheral blood mononuclear cells (PBMC) as a factor that enhances differentiation of pre-B cells in synergy with interleukin 7 (IL-)7 and stem cell factor.[1] Visfatin is mainly produced in visceral white adipose tissues, and shows an insulin-like effect by binding to insulin receptors.[2] Generally, visfatin is regarded as an adipokine, and elevated levels of serum visfatin in patients with type 2 diabetes,[3] and obesity,[4] have been reported. Interestingly, in visceral adipose tissues, macrophages seem to be the major source of visfatin.[5]

Visfatin is also produced by peripheral blood neutrophils upon stimulation by inflammatory factors such as lipopolysaccharide and tumour necrosis factor α (TNFα).[6] In addition, Nowell *et al* reported that IL-6 regulated visfatin production in synovial fibroblasts.[7] By contrast, visfatin has been shown to induce production of inflammatory molecules such as TNFα, IL-1β and IL-6.[8 9]

We measured the expression of the visfatin gene in synovial tissues (ST), PBMC and peripheral blood granulocytes (PBG) in patients with rheumatoid arthritis (RA).

cDNA from ST (22 RA, 17 osteoarthritis), PBMC and PBG (21 RA, 17 healthy controls (HC)) were used. Visfatin gene expression was analysed by reverse transcriptase (RT)-PCR. Plasma visfatin concentration was measured using Human Visfatin C-Terminal EIA Kit (Phoenix Pharmaceuticals, Burlingame, California, USA).

Results confirmed that visfatin gene expression is significantly higher than controls in ST, PBMC and PBG (fig 1).

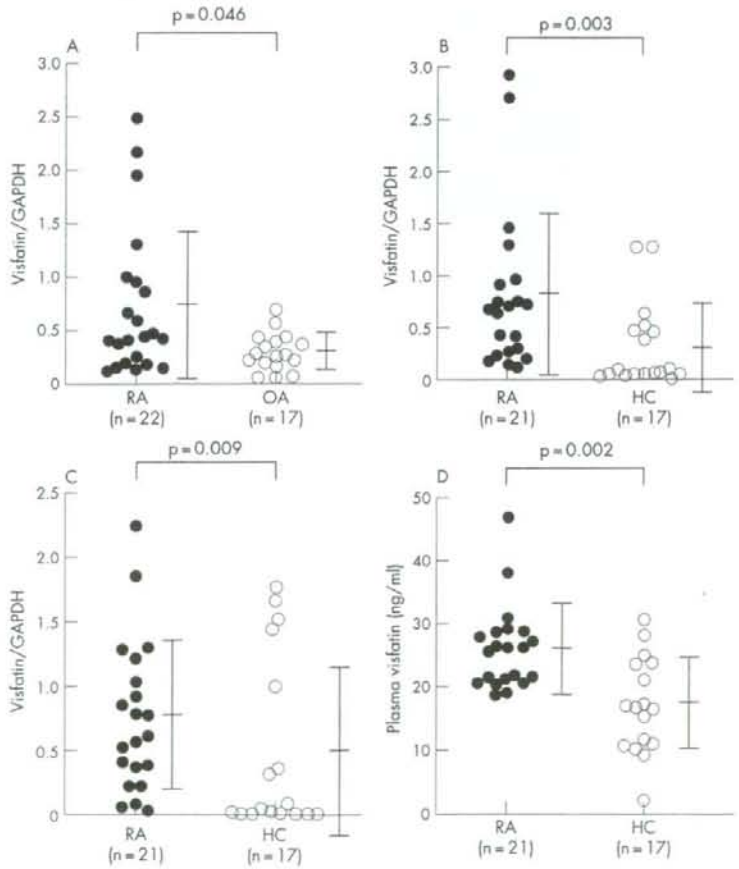

Figure 1 Visfatin (pre-B cell colony enhancing factor) gene expression and plasma visfatin concentration in patients with rheumatoid arthritis. Visfatin gene expression was measured by reverse transcriptase (RT)-PCR and was compensated with glyceraldehyde-2-phosphate dehydrogenase gene expression. Plasma visfatin concentration was measured by enzyme immunoassay. Statistical analyses by Mann–Whitney U test. Bars indicate mean (SD). A. Visfatin gene expression in synovial tissues. B. Visfatin gene expression in peripheral blood mononuclear cells. C. Visfatin gene expression in peripheral blood granulocytes. D. Plasma visfatin concentration. RA: rheumatoid arthritis. OA: osteoarthritis. GAPDH: glyceraldehyde-2-phosphate dehydrogenase. HC: healthy controls.

Plasma visfatin concentration in patients with RA was also significantly higher than that in HC (fig 1). A significant relationship between expressions of visfatin and IL-6 genes ($\rho = 0.514$, $p = 0.022$, by Spearman rank correlation), and a tendency towards a positive relationship between visfatin and TNFα genes ($\rho = 0.413$, $p = 0.065$, by Spearman rank correlation), were observed in PBMC of RA patients. No such relationship was observed in PBG or ST. No significant relationship was observed between expression of the visfatin gene in ST, PBMC or PBG, and clinical parameters including serum C-reactive protein (CRP), erythrocyte sedimentation rate (ESR), rheumatoid factor (RF), MMP-3 and white blood cell count. In RA patients, plasma visfatin concentration tended to correlate with visfatin gene expression in PBMC ($\rho = 0.344$, $p = 0.133$, by Spearman rank correlation). Plasma visfatin concentration was significantly related with serum RF ($\rho = 0.556$, $p = 0.026$ by Spearman rank correlation), and tended to have some relationship with ESR ($\rho = 0.434$, $p = 0.133$, by Spearman rank correlation).

A recent study by Otero *et al* showed that plasma visfatin levels are increased in patients with RA.[10] We have shown in this study that mRNA levels of visfatin are significantly increased in ST, PBMC and PBG of RA patients. Thus, in addition to adipose tissues, peripheral blood leukocytes and ST may serve as a source of visfatin in patients with RA.

Our results imply that visfatin is an active player in the inflammatory process of RA. Visfatin may become a candidate target for future therapies for patients refractory to conventional biologics.

H Matsui, A Tsutsumi, M Sugihara, T Suzuki, K Iwanami, M Kohno, D Goto, I Matsumoto, S Ito, T Sumida

Division of Clinical Immunology, Major of Advanced Biomedical Applications, Graduate School of Comprehensive Human Science, University of Tsukuba, Tsukuba, Japan

Correspondence to: A Tsutsumi, Division of Clinical Immunology, Major of Advanced Biomedical Applications, Graduate School of Comprehensive Human Science, University of Tsukuba, 1-1-1 Tennodai, Tsukuba 305-8575, Ibaraki, Japan; atsutsum@md.tsukuba.ac.jp

Competing interests: None declared.

Accepted 30 July 2007

Ann Rheum Dis 2008;**67**:571–572. doi:10.1136/ard.2007.077578

REFERENCES

1. **Samal B,** Sun Y, Stearns G, Xie C, Suggs S, McNiece I. Cloning and characterization of the cDNA encoding a novel human pre-B-cell colony-enhancing factor. *Mol Cell Biol* 1994;**14**:1431–7.
2. **Fukuhara A,** Matsuda M, Nishizawa M, Segawa K, Tanaka M, Kishimoto K, *et al*. Visfatin: a protein secreted by visceral fat that mimics the effects of insulin. *Science* 2005;**307**:426–30.
3. **Chen MP,** Chung FM, Chang DM, Tsai JC, Huang HF, Shin SJ, *et al*. Elevated plasma level of visfatin/pre-B cell colony-enhancing factor in patients with type 2 diabetes mellitus. *J Clin Endocrinol Metab* 2006;**91**:295–9.
4. **Berndt J,** Kloting N, Kralisch S, Kovacs P, Fasshauer M, Schon MR, *et al*. Plasma visfatin concentrations and fat depot-specific mRNA expression in humans. *Diabetes* 2005;**54**:2911–6.
5. **Curat CA,** Wegner V, Sengenes C, Miranville A, Tonus C, Busse R, *et al*. Macrophages in human visceral adipose tissue: increased accumulation in obesity and a source of resistin and visfatin. *Diabetologia* 2006;**49**:744–7.
6. **Jia SH,** Li Y, Parodo J, Kapus A, Fan L, Rotstein OD, *et al*. Pre-B cell colony-enhancing factor inhibits neutrophil apoptosis in experimental inflammation and clinical sepsis. *J Clin Invest* 2004;**113**:1318–27.
7. **Nowell MA,** Richards PJ, Fielding CA, Ognjanovic S, Topley N, Williams AS, *et al*. Regulation of pre-B cell colony-enhancing factor by STAT-3-dependent interleukin-6 trans-signalling: implications in the pathogenesis of rheumatoid arthritis. *Arthritis Rheum* 2006;**54**:2084–95.
8. **Ognjanovic S,** Tashima LS, Bryant-Greenwood GD. The effects of pre-B-cell colony-enhancing factor on the human fetal membranes by microarray analysis. *Am J Obstet Gynecol* 2003;**189**:1187–95.
9. **Moschen AR,** Kaser A, Enrich B, Mosheimer B, Theurl M, Niederegger H, *et al*. Visfatin, an adipocytokine with proinflammatory and immunomodulating properties. *J Immunol* 2007;**178**:1748–58.
10. **Otero M,** Lago R, Gomez R, Lago F, Dieguez C, Gomez-Reino JJ, *et al*. Changes in plasma levels of fat-derived hormones adiponectin, leptin, resistin and visfatin in patients with rheumatoid arthritis. *Ann Rheum Dis* 2006;**65**:1198–201.

Eosinophilic fasciitis and myositis: use of imaging modalities for diagnosis and monitoring

Eosinophilic fasciitis (EF) is a systemic inflammatory rheumatic disease first described by Shulman in 1974. EF is characterised by soft tissue swelling and pain, mostly located in the lower limbs. Blood eosinophilia is frequently found, but the creatinkinase is usually normal. Biopsy of both the fascia and the adjacent muscle is an established diagnostic tool.[1] Inflammation, oedema, thickening, and sclerosis of the fascia are hallmarks of EF, and the cellular infiltrate consists of lymphocytes, plasma cells, histiocytes, and eosinophils. By contrast, ultrasound has not been considered important for the diagnosis of EF to date.

We report here on the case of a 49-year-old female patient that came to our hospital because of pain in her calves that was mainly felt after physical exercise. There was no history of other symptoms indicating a rheumatic disease, or of medication or other diseases. The main clinical finding was pain and swelling in the calves that increased upon local pressure. Infectious causes of the condition were ruled out. Laboratory tests were normal. A soft tissue sonography showed a halo and a septal effusion of the calves (fig 1A,B). An MRI scan showed oedematous changes in the calf muscles (fig 1C,D). A biopsy was performed and analysed in laboratory specialised in neuromuscular diseases. The histological results provided evidence of severe eosinophilic fasciitis and muscle necrosis as described[6] (fig 1E–J).

In relation to the biopsy result, it was astonishing that there was no CK elevation despite the histological evidence of muscle necrosis. Very few cases of eosinophilic fasciitis and myositis without blood eosinophilia and elevation of the creatin kinase have been reported.[10]

The patient was initially treated with high doses of prednisolone,[3] which was then consecutively tapered. Hydroxychloroquine was started at a dosage of 200 mg twice a day as recommended.[8 9] After 1 week of therapy, the patient was clearly improved. Sonography of the calves was now normal and a control MRI showed only some fluid in the muscle septum.

This case deserves attention because eosinophilic fasciitis is a rather infrequent rheumatic condition that may not be easy to diagnose, especially when eosinophilia is absent. On the basis of the ultrasound finding described here, we think that this technique—which is relatively easy to perform—should have a role in the differential diagnosis of soft tissue pain. An important role for imaging has also been proposed by others.[2 4 5 7]

F Dybowski,[1] E Neuen-Jacob,[2] J Braun[1]

[1] Rheumazentrum Ruhrgebiet, St. Josef Krankenhaus, Herne, Germany;
[2] Neuropathologisches Institut Universitätsklinik, Düsseldorf, Germany

The American Journal of Pathology, Vol. 173, No. 6, December 2008

DOI: 10.2353/ajpath.2008.080314

Immunopathology and Infectious Diseases

Increased Foxp3$^+$ CD4$^+$ Regulatory T Cells with Intact Suppressive Activity but Altered Cellular Localization in Murine Lupus

Jun Abe,* Satoshi Ueha,* Jun Suzuki,*† Yoshiaki Tokano,† Kouji Matsushima,* and Sho Ishikawa*

From the Department of Molecular Preventive Medicine, Graduate School of Medicine, University of Tokyo, Tokyo, and the Department of Rheumatology,† School of Medicine, Juntendo University, Tokyo, Japan*

Foxp3$^+$ CD4$^+$ regulatory T (T_{reg}) cells play a pivotal role in the maintenance of dominant self tolerance. Understanding how the failures of immune control by T_{reg} cells are involved in autoimmune diseases is important for the development of effective immunotherapies. In the present study, we analyzed the characteristics of endogenous T_{reg} cells in (NZB × NZW) F1 (BWF1) mice, a murine model of systemic lupus erythematosus. Unexpectedly, T_{reg} number and frequency in aged BWF1 mice with developing lupus nephritis were increased, not decreased, and *in vitro* suppressive activity in lymphoid organs was intact. In addition, T_{reg} cells trafficked to target organs because cells were present in the kidney and lung. T_{reg} cells of aged BWF1 mice exhibited altered localization within lymph organs, however, and an altered phenotype, with higher expression levels of chemokine receptors and activation markers, suggesting a highly activated cellular state. Notably, the expression levels of costimulatory molecules were also markedly enhanced in the T_{reg} cells of aged BWF1 mice. Furthermore, T_{reg} cells of BWF1 mice did not show any suppressive effects on antibody production *in vitro*. Taken together, we conclude that T_{reg} cells in BWF1 mice are not predisposed to functional incompetence but rather are present in a highly activated state. (Am J Pathol 2008, 173:1682–1692; DOI: 10.2353/ajpath.2008.080314)

Systemic lupus erythematosus (SLE) is an autoimmune disease of unknown etiology characterized by a massive production of autoantibodies against various nuclear antigens. The deposit of immune complexes in the target organs, ie, skin, kidney, lung, joints, and central nervous system, is thought to cause fatal dysfunction of the body system. (NZB × NZW) F1 (BWF1) is a mouse strain that has been widely used as a model for SLE since the 1960s. These mice spontaneously develop severe autoimmune disease highly resembling human SLE in terms of serological and hematological abnormalities, and severe nephritis accompanying massive production of antinuclear antibodies.[1]

Reconstitution of SCID (severe combined immunodeficiency) mice with cultured pre-B cells of BWF1 mice recapitulates many symptoms of the disease of BWF1 mice. Cultured pre-B cells alone, however, are not sufficient to fully reproduce the disease.[2] These data suggest that cellular subset(s) in addition to B cells are necessary for the development of the lupus-like syndrome of BWF1 mice, although abnormalities of the immune system predominantly lie within B cells. One of the possible candidates is CD4$^+$ T cells, because depletion of CD4$^+$ T cells with anti-CD4 antibody from 5 months old, slightly before the disease onset, prevents the development of the disease.[3,4] CD4$^+$ T cells are, therefore, also required for the development of the disease in BWF1 mice, possibly by providing help for the production of high-affinity autoantibodies.

Studies in this decade have clearly shown the key roles of naturally occurring regulatory T (T_{reg}) cells in the maintenance of dominant self tolerance of the immune system.[5] T_{reg} cells in normal mice are mostly of thymic origin and are considered to be autoreactive T-cell clones that have bypassed negative selection by unknown mechanism(s).[6] There also exists T_{reg} cells of extra-thymic origin induced from conventional T cells during immune responses,[7] although the underlying mechanisms of this

Supported by the Long-Ranged Research Initiative of the Japan Chemical Industry Association and the Ministry of Health, Labor, and Welfare of Japan.

Accepted for publication September 9, 2008.

Supplemental material for this article can be found on http://ajp.amjpathol.org.

Address reprint requests to Sho Ishikawa, 7-3-1, Hongo, Bunkyo-ku, Tokyo, 113-0033, Japan. E-mail: yamasho@m.u-tokyo.ac.jp.

process are still unclear. Foxp3, a member of forkhead-box family of transcription factors, is specifically expressed in the whole life of T_{reg} cells and programs their functional properties.[8–10] In contrast to the previously used marker CD25 or combination of CD25 and CD62L, expression of Foxp3 is specific for T_{reg} cells, and thus can be used for the definitive identification of these cells.[11] Immunoregulatory function of T_{reg} cells is dependent on Foxp3 and genetic deficiency of *Foxp3* causes fatal organ-specific autoimmune disease because of the lack of functional T_{reg} cells.[12–14] Furthermore, many groups have reported the reduced number and/or function of T_{reg} cells in both organ-specific and systemic autoimmune diseases.[15]

A recent study has shown that the decreased frequency of T_{reg} cells in the peripheral blood was associated with disease activity in SLE patients.[16] Frequency of T_{reg} cells identified as $CD25^+$ $CD62L^{hi}$ $CD4^+$ T cells in the spleen was also decreased in aged BWF1 mice.[17] Accordingly, adoptive transfer of *in vitro*-expanded T_{reg} cells, or administration of histone-derived peptides or peptides derived from the complementarity-determining region 1 of anti-double-strand DNA immunoglobulin has been shown to ameliorate the disease in BWF1 mice by a mechanism involving T_{reg} cells.[17–20] These studies suggest that the function of endogenous T_{reg} cells is, at least partially, abrogated by unidentified mechanisms in BWF1 mice.

Despite the effort to develop therapeutic methods involving T_{reg} cells, their nature in BWF1 mice remains unclear. Here we performed a detailed characterization of T_{reg} cells in BWF1 mice using Foxp3 as their marker. Our results demonstrated that aged BWF1 mice had increased frequency and number of T_{reg} cells with apparently normal function, but with an activated phenotype including enhanced expression of co-stimulatory molecules and altered localization.

Materials and Methods

Mice

Female 6- to 8-week-old BWF1 and BALB/c mice were purchased from Japan SLC (Shizuoka, Japan) and were kept under specific pathogen-free conditions in the animal facility of our laboratory until analysis. Mice were used at 6 to 10 or 32 to 40 weeks of age as young or aged, respectively. All animal experiments were approved by the animal care committee of The University of Tokyo.

Antibodies

Monoclonal anti-mouse CD4 (clone RM4-5), CD5 (55-7.3), CD8α (53-6.7), CD11b (M1/70), CD16/32 (2.4G2), CD19 (1D3), CD23 (B3B4), CD25 (7D4), CD43 (S7), CD44 (IM7), CD45 (30-F11), CD45R (RA3-6B2), CD62L (MEL-14), CD69 (H1.2F3), CD90.2 (53-2.1), CD103 (M290), OX40 (OX-86), CXCR4 (2B11/CXCR4), CCR5 (C34-3448), NK1.1 (PK136), TER-119 (TER-119), and streptavidin were purchased from BD Biosciences (San Diego, CA); monoclonal anti-mouse 4-1BB (17B5), ICOS (7E.17G9), F4/80 (BM8), CCR7 (4B12), and Foxp3 (FJK-16s) were purchased from eBioscience (San Diego, CA); monoclonal anti-mouse CXCR3 (220803) was purchased from R&D Systems (Minneapolis, MN). Antiserum raised against mouse type IV collagen was purchased from LSL (Tokyo, Japan). Details of monoclonal anti-mouse CCR4 antibody (clone 2G11) will be described elsewhere by Nagakubo and colleagues.[21,22]

Cell Isolation

Single cell suspensions of the thymus, spleen, and lymph nodes were prepared by passing the tissue through a cell strainer (BD Bioscience). Single cell suspension of the kidney and lung were prepared by dissociating the tissue with collagenase D (Roche, Basel, Switzerland). Mononuclear cells in the kidney and lung were isolated from the single cell suspension by Percoll (Invitrogen, Carlsbad, CA) gradient centrifugation. $CD25^+$ $CD4^+$ T cells were isolated from the single cell suspension of various organs by magnetic enrichment of $CD25^+$ cells followed by fluorescence-activated cell sorting with the Epics Altra cell sorter (Beckman Coulter, Fullerton, CA). $CD25^-$ $CD4^+$ T cells were isolated from the single cell suspension of spleen by magnetic depletion of the cells positive for CD8α, CD11b, CD25, B220, CD138, NK1.1, or TER-119. B1 cells were isolated from peritoneal lavage cells by magnetic depletion of the cells positive for CD23, Thy-1.2, or F4/80. B2 cells were isolated from spleen by magnetic depletion of the cells positive for CD43, Thy-1.2, or TER-119. All procedures involving magnetic isolation were performed with an autoMACS system (Miltenyi Biotec, Bergisch Gladbach, Germany).

Flow Cytometry

Cells were incubated with fluorochrome- or biotin-labeled antibodies for 20 minutes at 4°C, following the blockade of FcγRII/III with unlabeled anti-CD16/32 for 10 minutes at 4°C; for the staining with biotin-labeled anti-CCR7, incubation after the blockade of Fc receptors was performed at 37°C. Biotin-labeled antibodies were visualized by further incubating with phycoerythrin-conjugated streptavidin for 15 minutes at 4°C. Staining of Foxp3 was performed according to the manufacturer's instructions. Data were collected using BD LSR II (BD Biosciences) and analyzed with FlowJo software (Tree Star, Ashland, OR).

Immunofluorescent Staining

Explanted tissues embedded in OCT compound were snap-frozen in liquid nitrogen and stored at −80°C until use. Six-μm-thick sections of frozen tissues were fixed with cold acetone for 10 minutes and rehydrated with phosphate-buffered saline (PBS) for 10 minutes at room temperature. Rehydrated sections were blocked for nonspecific binding of proteins with Blocking One (Nacalai Tesque, Kyoto, Japan) for 20 minutes at room temperature and incubated with unlabeled or biotinylated anti-

Table 1. Primers and Probes for Real-Time PCR

Gene	Sense	Probe	Antisense
CCL19	5'-GAAAGCCTTCCGCTACCTTCT-3'	5'-CCCATCCCGGCAATCCTGTTCTTA-3'	5'-CCCTTAGTGTGGTGAACACAA-CA-3'
CCL21	5'-GGCTATAGGAAGCAAGAACCAA-GT-3'	5'-TTACTTCTACCGACGTCCCACGGA-3'	5'-TCAGGCTTAGAGTGCTTCCG-3'
CXCL9	5'-TGATAAGGAATGCACGATGCTC-3'	5'-AGCCGAGGCACGATCCACTACAAA-TC-3'	5'-TTCCTTGAACGACGACGACTTT-3'
CXCL10	5'-CGTCATTTTCTGCCTCATCCT-3'	5'-AAGCTTGAAATCATCCCTGCGAG-CC-3'	5'-TGGTCTTAGATTCCGGATTCAG-3'
CXCL12	5'-GCTCTGCATCAGTGACGGTAA-3'	5'-ATCGCCAGAGCCAACGTCAAGCAT-CT-3'	5'-AGCCGTGCAACAATCTGAAG-3'
GAPDH	5'-AGTATGACTCCACTCACGGCAA-3'	5'-AACGGCACAGTCAAGGCCGAGAAT-3'	5'-TCTCGCTCCTGGAAGATGGT-3'

bodies, or antisera for 60 minutes at room temperature. Sections were then incubated with Alexa Fluor-labeled anti-Ig secondary antibodies or streptavidin (Invitrogen) for 30 minutes at room temperature. After the staining, sections were fixed with phosphate-buffered 4% paraformaldehyde for 10 minutes at room temperature and were mounted with Prolong Gold Antifade Reagent (Invitrogen). Specimens were observed under IX70 confocal laser-scanning microscopy (Olympus, Tokyo, Japan).

Quantification of Histological Analysis

Images obtained from confocal microscopic observation were processed with Win ROOF software (Mitani Corporation, Fukui, Japan), and the number of the signals was counted manually or automatically using Win ROOF software.

In Vitro *Proliferation and Suppression Assay*

2×10^4 cells/well of purified $CD25^-$ $CD4^+$ T cells were stimulated with 2 μg/ml of concanavalin A (Sigma-Aldrich, St. Louis, MO) and 8×10^4 cells/well of mitomycin-C (Sigma-Aldrich)-treated Thy1.2$^-$ splenocytes with or without titrated number of $CD25^+$ $CD4^+$ T cells were incubated in RPMI 1640 medium supplemented with 10% heat-inactivated fetal bovine serum, 10 mmol/L HEPES, 55 μmol/L 2-mercaptoethanol, 100 U/mL penicillin, and 100 μg/mL streptomycin in a round-bottom 96-well plate for 72 hours at 37°C. $CD25^+$ $CD4^+$ T cells were cultured under the same conditions to measure their proliferative capacity in the absence of $CD25^-$ $CD4^+$ T cells. Cells were pulsed with 1 μCi/well [^{3}H-methyl]-thymidine (GE Health Care, Buckinghamshire, UK) for the last 6 to 8 hours of the culture, and proliferation was measured by cpm value of the harvested cells. Suppressive activity of $CD25^+$ $CD4^+$ T cells was expressed as percent suppression[23] calculated as following: $100 \times$ [cpm (responder) − cpm($CD25^+$ + $CD25^-$)]/cpm(responder).

In Vitro *Antibody Production Assay*

In vitro antibody production by B cells was analyzed as previously described[24] with several modifications. Briefly, 2×10^5 B1 or B2 cells isolated from young or aged BWF1 mice and equal numbers of $CD25^-$ $CD4^+$ T cells isolated from the spleen of young or aged BWF1 mice were cultured with or without 1×10^5 $CD25^+$ $CD4^+$ T cells in supplemented RPMI 1640 medium for 5 days at 37°C. The concentration of IgG antibody in the culture supernatant was measured by enzyme-linked immunosorbent assay using a Mouse IgG quantitation kit (Bethyl, Montgomery, TX).

Preparation of cDNA and Real-Time Polymerase Chain Reaction (PCR)

Mice were perfused with 30 mL of PBS, and spleen, lymph nodes, kidney, and lung were excised. Tissues were homogenated with TRIzol reagent (Invitrogen), and purified total RNA was reverse-transcribed with a high-capacity cDNA reverse transcription kit (Applied Biosystems, Foster City, CA). Real-time PCR was performed with an ABI Prism 7500 (Applied Biosystems) using primers and Taq Man probes listed in Table 1.

Statistical Analysis

Statistical significance of the difference between data sets was analyzed by Welch's unpaired *t*-test for the comparison of two groups or by one-way analysis of variance with Bonferroni's multiple comparison test for more than three groups. $P < 0.05$ was considered to be statistically significant.

Results

Increased Number and Frequency of T_{reg} Cells in Aged BWF1 Mice

Suppressive activity of T_{reg} cells is strongly correlated with the expression of Foxp3.[11] To clarify whether an increase or decrease in the frequency and/or number of T_{reg} cells exists, we analyzed the population of $Foxp3^+$ $CD4^+$ T cells by flow cytometry. We found that aged BWF1 mice had substantially increased frequency (Figure 1A) and number (Figure 1B) of $Foxp3^+$ $CD4^+$ T cells in the lymphoid organs compared with young BWF1 mice. A recent study has shown an age-dependent increase in $CD25^-$ $Foxp3^+$ $CD4^+$ T cells in 24-month-old normal mice,[25] but increased $Foxp3^+$ $CD4^+$ T cells in aged BWF1 mice was not merely an age-dependent event be-

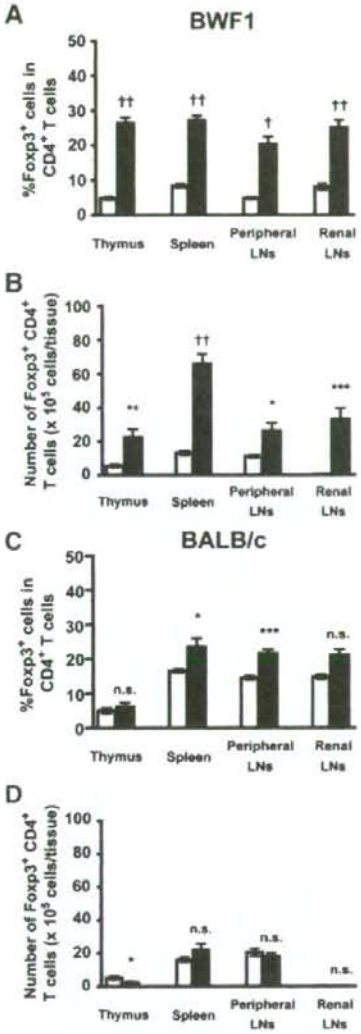

Figure 1. Increased Foxp3$^+$ CD4$^+$ T_{reg} cells in aged BWF1 mice. Frequency (**A**, **C**) and number (**B**, **D**) of Foxp3$^+$ CD4$^+$ T cells within thymus, spleen, peripheral LNs (inguinal, axillary, brachial, submandibular, and cervical), and renal lymph node of BWF1 (**A**, **B**) or BALB/c (**C**, **D**) mice were analyzed by flow cytometry. Data were presented as mean ± SEM ($n = 4$ to 9 for each group). Open bar, young; filled bar, aged. Statistical significance of the difference between young and aged mice was analyzed by Welch's unpaired *t*-test. $^*P < 0.05$, $^{**}P < 0.01$, $^{***}P < 0.005$, $^{\dagger}P < 0.0005$, $^{\dagger\dagger}P < 0.0001$.

cause age-matched BALB/c mice did not show a marked increase in Foxp3$^+$ CD4$^+$ T cells (Figure 1, C and D).

CD25$^+$ CD4$^+$ T Cells Showed Normal Suppressive Activity Both in Young and Aged BWF1 Mice

Valencia and colleagues[16] reported a decreased suppressive activity of CD25$^+$ CD4$^+$ T cells in SLE patients, possibly because of the lower proportion of Foxp3$^+$ cells among CD25$^+$ CD4$^+$ T cells. This result, however, does not exclude the possibility that a functional defect intrinsic to T_{reg} cells exists as well. To test the functional competency of T_{reg} cells of BWF1 mice, we performed an *in vitro* suppression assay. Because Foxp3 expression could be detected only in permeabilized cells, we used CD25$^+$ CD4$^+$ T cells as a surrogate for Foxp3$^+$ CD4$^+$ T cells. Concurrent with the high proportion of Foxp3$^+$ cells among CD25$^+$ CD4$^+$ T cells even after disease onset (Figure 2A), CD25$^+$ CD4$^+$ T cells isolated from the spleen and lymph nodes of both young and aged BWF1 mice did not proliferate on stimulation (Figure 2B) and showed suppressive activity (Figure 2C). Furthermore, CD25$^+$ CD4$^+$ T cells isolated from the kidney (Figure 2C) and lung (data not shown), ie, the target organs, of aged BWF1 mice also showed suppressive activity comparable to those from the spleen and lymph nodes. CD25$^+$ CD4$^+$ T cells of thymus or lymph nodes showed similar suppressive activity (data not shown). We did not note a significant difference in the suppressive activity between young and aged, or lymphoid and nonlymphoid CD25$^+$ CD4$^+$ T cells in BWF1 mice at any dose of CD25$^+$ CD4$^+$ T cells. Taken together, our data suggest that aged BWF1 mice have an expanded pool size of T_{reg} cells with intact suppressive activity.

T_{reg} Cells Infiltrated into the Target Organs

Defective migration into the site of inflammation is known to impair the *in vivo* suppressive activity of T_{reg} cells even if they were functionally competent *in vitro*.[26] Because our data indicated that T_{reg} cells of BWF1 mice have intact suppressive activity *in vitro*, we asked whether T_{reg} cells in aged BWF1 mice infiltrated into the target organs, ie, kidney and lung. Flow cytometric analysis of mononuclear cells within the target organs revealed that Foxp3$^+$ as well as Foxp3$^-$ CD4$^+$ T cells infiltrated into these organs, and that the frequency of Foxp3$^+$ cells in CD4$^+$ T cells was comparable to that in the lymph nodes of normal mice[11] (18.76 ± 3.79% in the kidney and 14.08 ± 2.50% in the lung). Foxp3$^+$ CD4$^+$ T cells infiltrated into the glomeruli, interstitium, and perivascular region of the kidney along with Foxp3$^-$ CD4$^+$ T cells (Figure 3B). Young BWF1 mice and nonautoimmune control mice did not show the infiltration of inflammatory cells (data not shown). Moreover, both Foxp3$^+$ and Foxp3$^-$ CD4$^+$ T cells were apparently distributed evenly within the infiltrating site of the target organs (Figure 3, A and C), indicating that clustering of these cells that were essential for T_{reg} cell-mediated suppression[26,27] would take place in the target organs as well as in the lymphoid organs.

Medullary Localization of T_{reg} Cells within the Thymus

The thymus, another target organ of the disease in BWF1 mice, is the major site of the development of T_{reg} cells.[6] Disruption of the architecture of the thymic medulla where development of T_{reg} cells occurs is known to impair that process.[28] To determine whether T_{reg} cells are properly

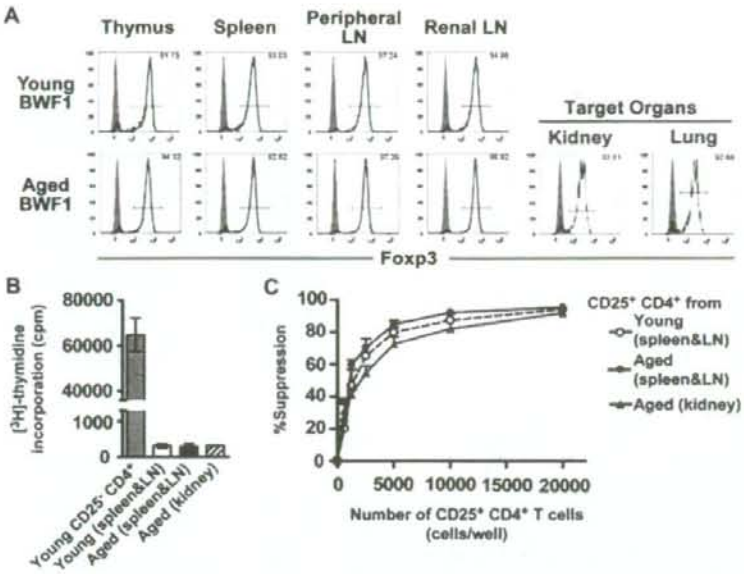

Figure 2. Suppressive activity of CD25$^+$ CD4$^+$ T cells. **A:** Representative profile of Foxp3 expression in CD25$^+$ CD4$^+$ T cells of young or aged BWF1 mice used for suppression assay ($n = 3$ for each group). Numbers in the histograms indicate the frequency of Foxp3$^+$ cells. Shaded histogram indicates isotype control. Note that CD25$^+$ CD4$^+$ T cells are highly enriched for Foxp3$^+$ T_{reg} cells. **B:** Proliferation of CD25$^+$ CD4$^+$ T cells isolated from the spleen and lymph nodes of young or aged BWF1 mice or from the target organs of aged BWF1 mice. Data are presented as mean ± SEM. **C:** *In vitro* suppressive activity of CD25$^+$ CD4$^+$ T cells isolated from the spleen and lymph nodes of young or aged BWF1 mice or from the kidney of aged BWF1 mice. Data were presented as mean + SEM. Differences between the three groups presented in the graph were not significant when analyzed by one-way analysis of variance with Bonferroni's multiple comparison test. A representative of three independent experiments that gave similar results is shown.

located within the thymus, we analyzed thymic sections by immunofluorescent staining. In BWF1 mice, thymic architecture is strongly affected by the disease,[4,29] but medullary localization of T_{reg} cells remained virtually unchanged even after the manifestation of severe nephritis (Figure 3, D and E). Localization of T_{reg} cells within the thymus is also confined to the medulla in BALB/c mice irrespective of their age (Supplemental Figure 1, A and B, see *http://ajp.amjpathol.org*).

Altered Distribution of T_{reg} Cells within the Secondary Lymphoid Organs of Aged BWF1 Mice

T_{reg} cells have to be located in the site of antigen presentation within the secondary lymphoid organs to make contacts with their target cells.[26,27] Because our analyses on the number, function, and site of the development of T_{reg} cells could not find any obvious defect, we examined the localization of T_{reg} cells within the secondary lymphoid organs of BWF1 mice. T_{reg} cells in aged BWF1 mice were located in the follicles and red pulp as well as periaortic lymphoid sheath in the spleen, whereas T_{reg} cells in young BWF1 mice were mostly located in the periaortic lymphoid sheath (Figure 3, F and G; Supplemental Figure 2, see *http://ajp.amjpathol.org*). Similar localization of T_{reg} cells were observed in the renal lymph node where T_{reg} cells were located in the follicles and medulla as well as paracortex in aged BWF1 mice, whereas the localization of T_{reg} cells in young BWF1 mice was relatively confined to paracortex (Figure 3, H and I; Supplemental Figure 2, see *http://ajp.amjpathol.org*). Such altered localization was not limited to T_{reg} cells, but was also seen in Foxp3$^-$ conventional T cells. In contrast, localization of T_{reg} cells in BALB/c mice was not altered with age and was similar to that of young BWF1 mice (Supplemental Figures 1, C–F, and 2, see *http://ajp.amjpathol.org*).

Changes in the Expression of Chemokine Receptors on T_{reg} Cells in Aged BWF1 Mice

Localization of T cells is tightly regulated by various chemokines and their receptors to achieve efficient induction of immune response or tolerance.[30] To elucidate the molecule(s) responsible for the altered localization of T_{reg} cells, we next analyzed the expression of chemokine receptors involved in the function of T_{reg} cells[31–34] by flow cytometry. Both Foxp3$^+$ and Foxp3$^-$ CD4$^+$ T cells in the spleen showed decreased CCR7 expression (Figure 4C) and enhanced CXCR4 expression (Figure 4E) in aged BWF1 mice. On the other hand, the expression level of CCR4, CCR5, and CXCR3 did not show marked difference between young and aged BWF1 mice (Figure 4, A, B, and D), except that CXCR3 expression was slightly enhanced on both Foxp3$^+$ and Foxp3$^-$ cells of aged BWF1 mice (Figure 4, F and H). These changes in the expression of chemokine receptors on CD4$^+$ T cells were not observed in BALB/c mice (Figure 4, G and I). Expression pattern of chemokine receptors on CD4$^+$ T cells in the target organs and lymph nodes was similar to that of splenic CD4$^+$ T cells (data not shown). Aged BWF1 mice showed a 5 to 7 fold decrease in the expression of CCL19, CCL21, and CXCL12, ligands for CCR7 and CXCR4, in the lymphoid organs (Supplemental Figure 3, see *http://ajp.amjpathol.org*). On the other hand, expression of CXCL9 and CXCL10, ligands for CXCR3, were increased 2- to 3-fold and 8- to 28-fold, respectively, in

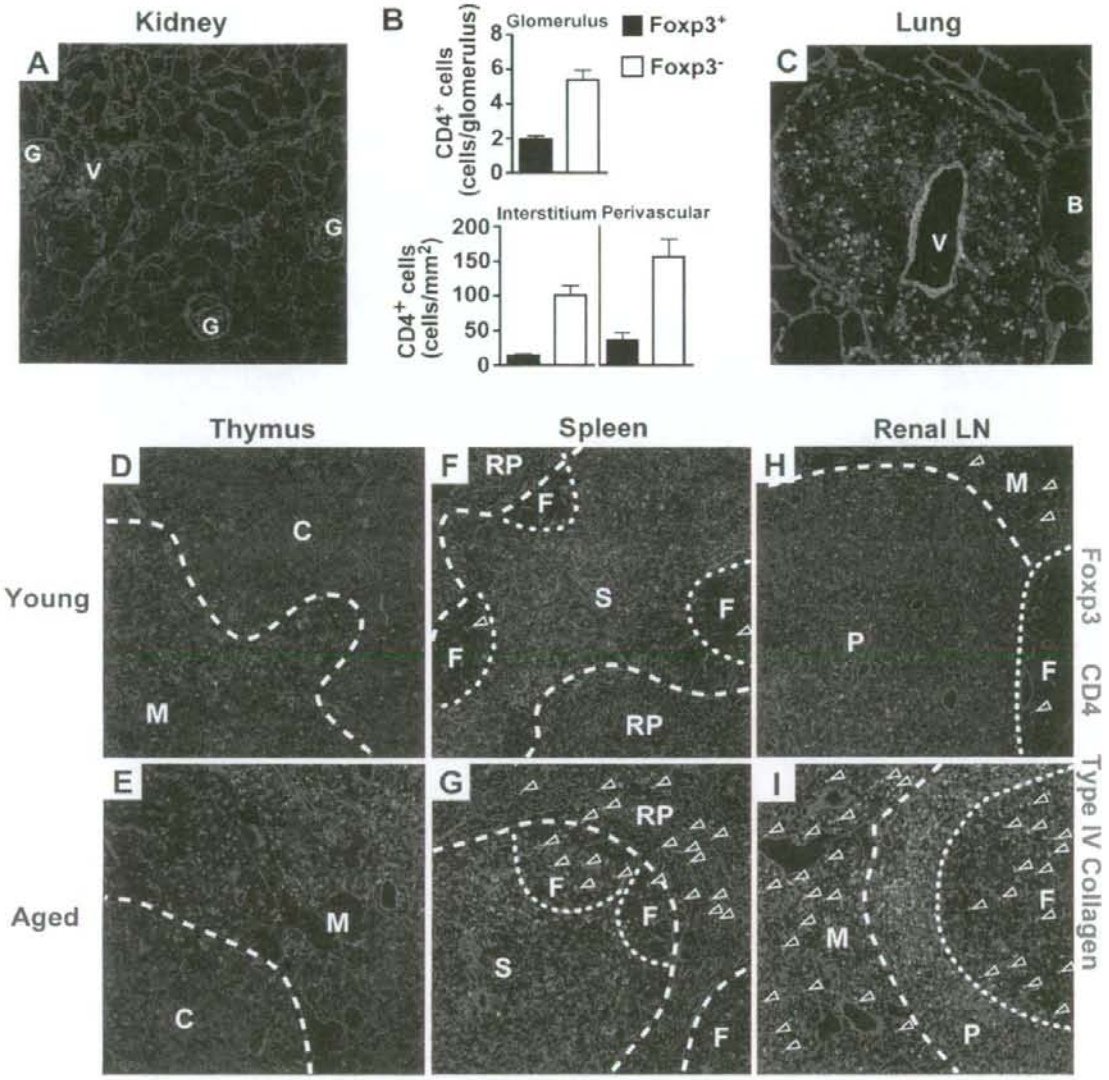

Figure 3. Altered localization of T_{reg} cells in aged BWF1 mice. **A–C:** Histological analysis of the kidney and lung of aged BWF1 mice ($n = 4$). **A** and **C:** Triple immunofluorescent staining of a 6-μm-thick cryosection of the kidney (**A**) and lung (**C**) of aged BWF1 mice with anti-Foxp3 (green), anti-CD4 (red), and anti-type IV collagen (blue). Green signal on the vascular endothelium and bronchus of the lung was also detected in isotype control (data not shown). Such nonspecific signal was not observed in $CD4^+$ cells. **B:** Summary of the number of $Foxp3^+$ (filled bar) and $Foxp3^-$ (open bar) $CD4^+$ T cells within renal compartments. Data were expressed as mean ± SEM. More than three fields were counted to calculate the mean value. **D–I:** Triple-immunofluorescent staining of 6-μm-thick cryosection of the thymus (**D**, **E**), spleen (**F**, **G**), and renal lymph node (**H**, **I**) of young (**D**, **F**, **H**) or aged (**E**, **G**, **I**) BWF1 mice with anti-Foxp3 (green), anti-CD4 (red), and anti-type IV collagen (blue). B, bronchus; C, cortex; F, follicle; G, glomerulus; M, medulla; RP, red pulp; P, paracortex; S, periaortic lymphoid sheath; V, blood vessel. **Arrowheads** in **D–I** indicate $Foxp3^+$ $CD4^+$ T cells located out of paracortex or periaortic lymphoid sheath. Representatives of the independent examination of four young and aged BWF1 mice are shown. Original magnifications, ×100.

the lymphoid organs and target organs, respectively (Supplemental Figure 3, see *http://ajp.amjpathol.org*).

Activated Phenotype of Both $Foxp3^+$ and $Foxp3^-$ $CD4^+$ T Cells in Aged BWF1 Mice

Altered localization of T_{reg} cells in aged BWF1 mice per se does not explain the cause of their failure to control the autoimmunity. We found that T_{reg} cells of aged BWF1 mice showed decreased expression of CD25 and CD62L (Figure 5, A, B, and I), in contrast to the enhanced or unaltered expression of activation markers CD44, CD69, and CD103 (Figure 5, C–E, and I). Various co-stimulatory molecules up-regulated on activation were reported to affect the function and/or number of T_{reg} cells,[35–37] therefore, we analyzed the expression of co-stimulatory molecules of

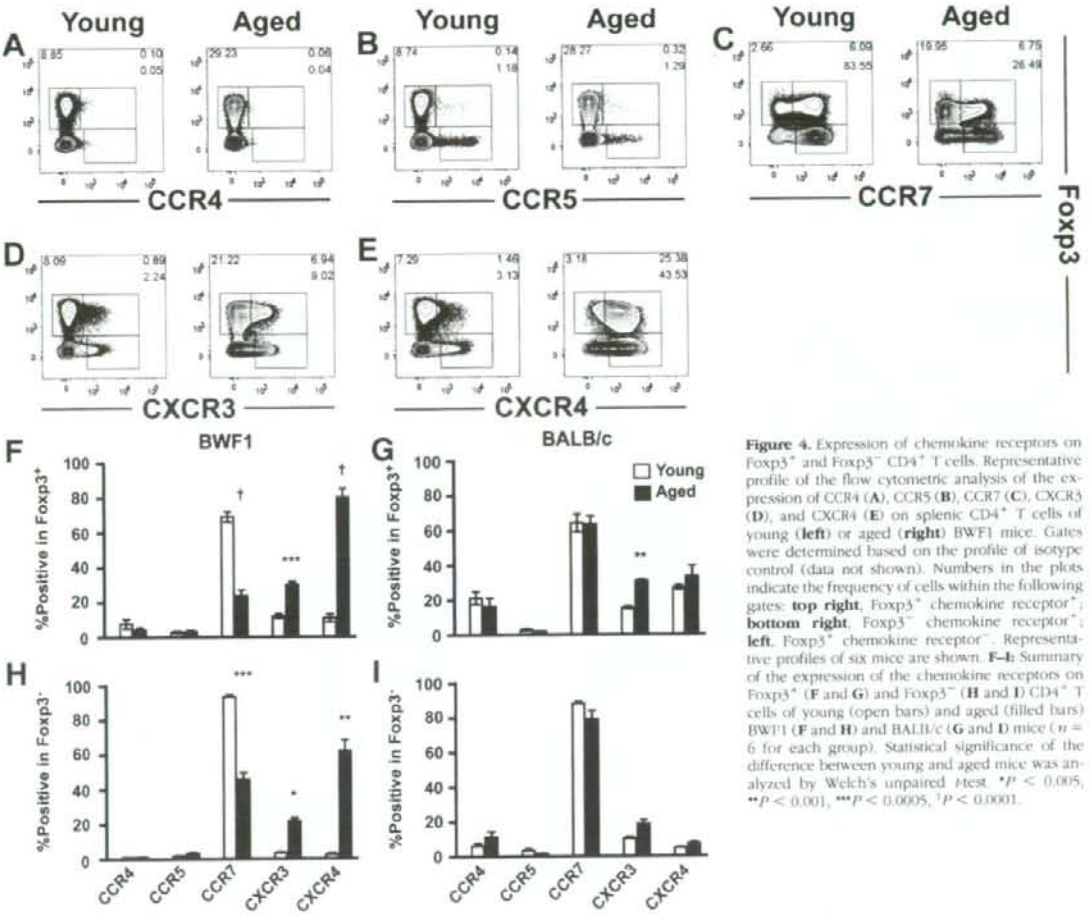

Figure 4. Expression of chemokine receptors on Foxp3$^+$ and Foxp3$^-$ CD4$^+$ T cells. Representative profile of the flow cytometric analysis of the expression of CCR4 (**A**), CCR5 (**B**), CCR7 (**C**), CXCR3 (**D**), and CXCR4 (**E**) on splenic CD4$^+$ T cells of young (**left**) or aged (**right**) BWF1 mice. Gates were determined based on the profile of isotype control (data not shown). Numbers in the plots indicate the frequency of cells within the following gates: **top right**, Foxp3$^+$ chemokine receptor$^+$; **bottom right**, Foxp3$^-$ chemokine receptor$^+$; **left**, Foxp3$^+$ chemokine receptor$^-$. Representative profiles of six mice are shown. **F–I:** Summary of the expression of the chemokine receptors on Foxp3$^+$ (**F** and **G**) and Foxp3$^-$ (**H** and **I**) CD4$^+$ T cells of young (open bars) and aged (filled bars) BWF1 (**F** and **H**) and BALB/c (**G** and **I**) mice (n = 6 for each group). Statistical significance of the difference between young and aged mice was analyzed by Welch's unpaired t-test. $^*P < 0.005$, $^{**}P < 0.001$, $^{***}P < 0.0005$, $^{\dagger}P < 0.0001$.

T_{reg} cells. Associated with their activated phenotype, costimulatory molecules OX40, 4-1BB, and ICOS were expressed on CD4$^+$ T cells in aged BWF1 mice at higher level than young BWF1 (Figure 5, F–I). Among them, expression of OX40 and ICOS was enhanced on both Foxp3$^+$ and Foxp3$^-$ T cells, whereas expression of 4-1BB was enhanced only on Foxp3$^+$ T_{reg} cells (Figure 5, I and K). Age-dependent alteration of surface phenotype in BALB/c mice was limited to slight changes in CD44 and CD62L (Figure 5, J and L).

Inability of T_{reg} Cells of BWF1 Mice to Suppress in Vitro IgG Antibody Production

Lastly, we assessed the impact of T_{reg} cells on the antibody production by B cells. Sekigawa and colleagues[24] demonstrated that CD4$^+$ T cells of aged BWF1 mice induced IgG antibody production of splenic B cells on stimulation with concanavalin A and lipopolysaccharide *in vitro*. We used this method with several modifications and found that CD25$^-$ CD4$^+$ T cells of aged, but not young, BWF1 mice induced IgG antibody production by B cells even in the absence of the stimuli (Figure 6 and data not shown). Because antibody production by B cells was totally dependent on the presence of CD4$^+$ T cells in this assay, we assumed that T_{reg} cells would suppress the antibody production by interfering with CD4 help. CD25$^+$ CD4$^+$ T cells, however, did not affect the amount of IgG antibody produced by B cells (Figure 6), demonstrating that T_{reg} cells of both young and aged BWF1 mice are unable to suppress IgG antibody production induced by CD4$^+$ T cells of aged BWF1 mice.

Discussion

Foxp3$^+$ CD4$^+$ T_{reg} cells play a pivotal role in the maintenance of dominant self tolerance, and lack of functional T_{reg} cells is associated with various autoimmune diseases. In contrast, our present study in a murine model of SLE revealed a substantially expanded pool size of T_{reg} cells with a phenotype suggesting their highly activated state, and their inability to suppress antibody production *in vitro*.

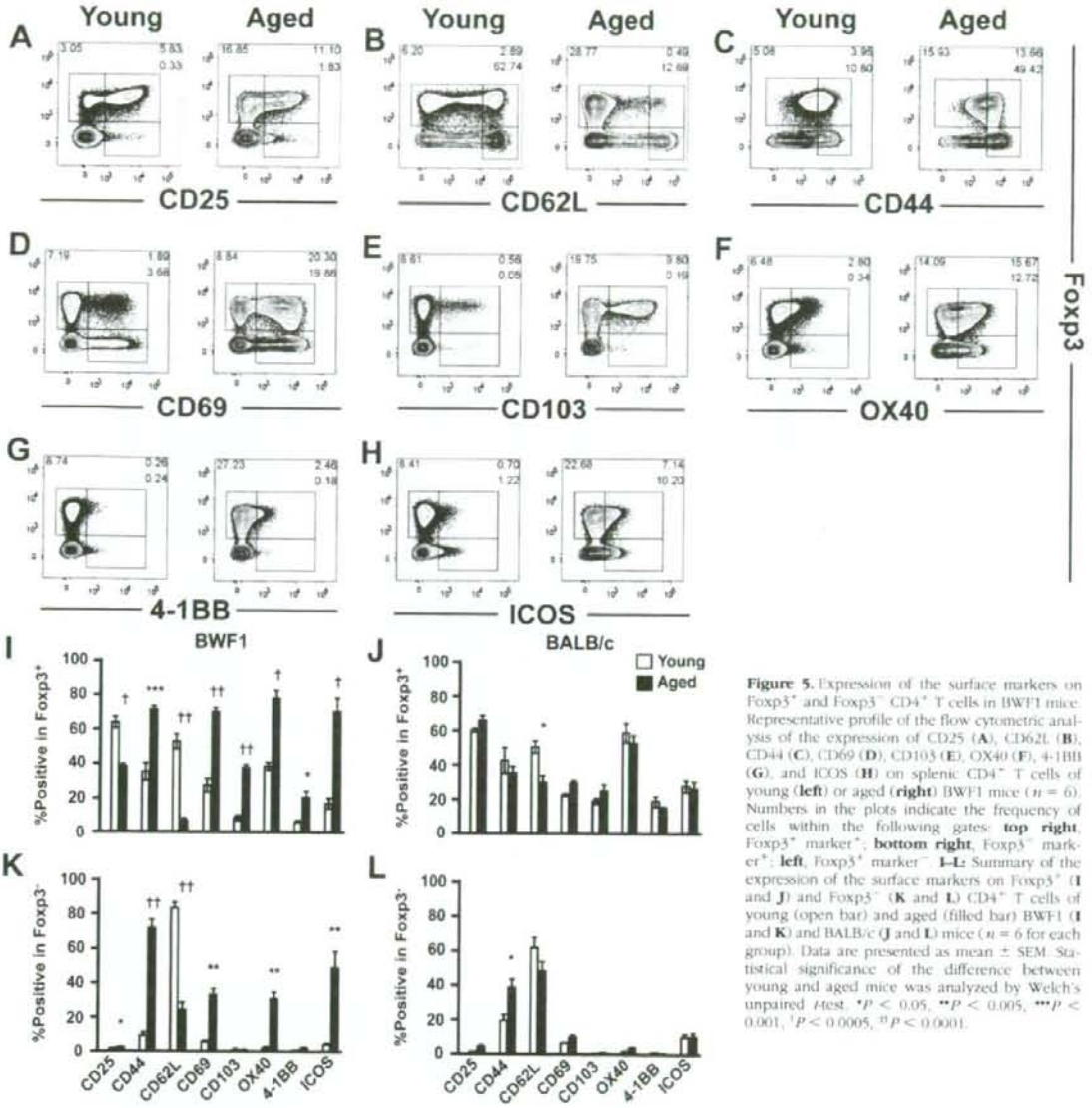

Figure 5. Expression of the surface markers on Foxp3$^+$ and Foxp3$^-$ CD4$^+$ T cells in BWF1 mice. Representative profile of the flow cytometric analysis of the expression of CD25 (**A**), CD62L (**B**), CD44 (**C**), CD69 (**D**), CD103 (**E**), OX40 (**F**), 4-1BB (**G**), and ICOS (**H**) on splenic CD4$^+$ T cells of young (**left**) or aged (**right**) BWF1 mice ($n = 6$). Numbers in the plots indicate the frequency of cells within the following gates: **top right**, Foxp3$^+$ marker$^+$; **bottom right**, Foxp3$^-$ marker$^+$; **left**, Foxp3$^+$ marker$^-$ **I–L:** Summary of the expression of the surface markers on Foxp3$^+$ (**I** and **J**) and Foxp3$^-$ (**K** and **L**) CD4$^+$ T cells of young (open bar) and aged (filled bar) BWF1 (**I** and **K**) and BALB/c (**J** and **L**) mice ($n = 6$ for each group). Data are presented as mean ± SEM. Statistical significance of the difference between young and aged mice was analyzed by Welch's unpaired *t*-test. $^*P < 0.05$, $^{**}P < 0.005$, $^{***}P < 0.001$, $^{\dagger}P < 0.0005$, $^{\ddagger}P < 0.0001$.

We could not detect any obvious defect in the suppressive activity of T_{reg} cells in BWF1 mice. In addition, localization of both T_{reg} cells and Foxp3$^-$ conventional CD4$^+$ T cells within the lymphoid organs was altered, but they showed concomitant migratory behavior. These data collectively suggest that T_{reg} cells in BWF1 mice had little defect in their function, and the failure of T_{reg} cells to control the disease might be predominantly caused by the extrinsic factors, such as cytokine milieu and co-stimulatory signals provided by antigen-presenting cells (APCs). On the other hand, it is reported that treatment of BWF1 mice with the T_{reg} cell-inducing molecules such as all-*trans*-retinoic acid or tolerogenic peptides delays or prevents the onset of murine lupus.[18–20,38] One possible explanation for the failure of T_{reg} cells to control the disease is that presence of T_{reg} cells capable of controlling the disease at an earlier stage is critical, as suggested by the previous reports in which induction of T_{reg} cells in BWF1 mice was conducted well before the onset of the disease. Another possibility is the antigen specificity of T_{reg} cells. La Cava and colleagues[19] showed that induction of T_{reg} cells specific for the peptide derived from anti-DNA antibody were associated with the therapeutic effect of this peptide in BWF1 mice. This report raises the possibility that endogenous T_{reg} cells in pre-diseased BWF1 mice lack population(s) with such antigen specificity, and expansion of the pool size of T_{reg} cells in aged BWF1 mice with severe nephritis does not